JOURNAL OF QUATERNARY SCIENCE (2023) 1–25 ISSN 0267-8179. DOI: 10.1002/jqs.3503

JQS Journal of Quaternary Science QRA Quaternary Research Association

Impacts of Early Holocene environmental dynamics on open-air occupation patterns in the Western Mediterranean: insights from El Arenal de la Virgen (Alicante, Spain)

JAVIER FERNÁNDEZ-LÓPEZ DE PABLO,[1]* ANA POLO-DÍAZ,[2] JOSÉ RAMÓN RABUÑAL,[1,3] MAGDALENA GÓMEZ PUCHE,[1] YOLANDA CARRIÓN MARCO,[4] ANA CANTÓ,[4] ROWAN MCLAUGHLIN,[5] CARLOS FERRER[6] and FRANCESC BURJACHS[7,8,9]

[1]I.U. de Investigación en Arqueología y Patrimonio Histórico (INAPH), University of Alicante, Carr. de San Vicente del Raspeig, s/n, San Vicente del Raspeig, Alicante, Spain
[2]Department of Geography, Prehistory and Archaeology, University of the Basque Country (UPV/EHU), Vitoria-Gasteiz, Spain
[3]Department of Archaeology and Heritage Studies, Aarhus University, Højbjerg, Denmark
[4]Department of Prehistory, Archaeology and Ancient History, University of Valencia, Valencia, Spain
[5]Maynooth, National University of Ireland, Kildare, Ireland
[6]Museu de Prehistòria de Valencia, Centro Cultural La Beneficència, Valencia, Spain
[7]ICREA, Institució Catalana de Recerca i Estudis Avançats, Barcelona, Catalunya, Spain
[8]Institut Català de Paleoecologia Humana i Evolució Social (IPHES), Zona Educacional 7 Campus Sescelades URV (Edifici W3), Tarragona, Spain
[9]Àrea de Prehistòria, Universitat Rovira i Virgili, Tarragona, Spain

Received 2 June 2022; Revised 10 January 2023; Accepted 16 January 2023

ABSTRACT: Open-air sites represent a fundamental proxy of the Early Holocene adaptive systems in the Iberian Peninsula. However, its research potential for the study of human–environmental interactions has been minimally explored. In this work, we present the results of an integrated research programme focused on open-area excavations at the Mesolithic site of Arenal de la Virgen (Alicante, Spain). Novel multi-scalar geoarchaeological and archaeo-stratigraphic studies, coupled with featured-based palaeobotanical analysis, were used to design an extensive radiocarbon dating programme and produce different Bayesian chronological models. Our results distinguish two different Mesolithic occupation phases, dating to 9.3–9.1 and 8.6–8.3k cal a BP respectively, consisting of combustion features and lithic scatters. The comparison of occupational dynamics with the nearby palaeoecological records of Salines and Villena indicated that both Mesolithic phases occurred under relatively stable environmental conditions. The second Mesolithic phase, however, ended during the onset of the 8.2k cal a BP climatic event, when sedimentation processes shifted from soil formation to accretion of aeolian sands. We demonstrate that the end of the Mesolithic occupations at Arenal de la Virgen coincides with the cessation of radiocarbon-dated activity in other open-air Postglacial sites in the central Mediterranean region of Iberia.

KEYWORDS: 8.2k cal a BP climatic event; geoarchaeology; Iberian Peninsula; Mesolithic; open-air sites; palaeoecology; radiocarbon dating

Introduction

The study of human responses to Early Holocene climatic and environmental dynamics has become a focal point in Quaternary research. This period witnessed both gradual, millennial-scale, changes and abrupt climatic events (ACEs), with a significant degree of regional variability in vegetation and hydrological patterns. The Iberian Peninsula (Fig. 1) is one of the areas of Europe where the impacts of Early to Middle Holocene environmental dynamics on human systems, especially the 8.2k cal a BP climatic event (Rohling and Pälike 2005), have been most extensively discussed (González-Sampériz *et al.*, 2009; Fernández-López de Pablo and Jochim 2010; Bicho *et al.*, 2010; Cortés *et al.*, 2012; García-Martínez de Lagrán *et al.*, 2016; Alday *et al.*, 2018; García-Escárzaga *et al.*, 2022).

The potential effects of the 8.2k cal a BP climatic event on Late Mesolithic occupation patterns were first proposed in the Central Ebro basin (González-Sampériz *et al.*, 2009). This area witnessed an intensification of aridity (a decrease of mesophytes and lower lake levels), which is thought to have negatively impacted the Mesolithic populations, forcing their migration to neighbouring Mediterranean areas of the Maestrazgo and the Upper Ebro valley (González-Sampériz *et al.*, 2009; Utrilla *et al.*, 2009). Subsequent research evaluated in detail this hypothesis through an interstratification analysis of occupation vs. sterile layers of the Mesolithic sequences of Botiquería dels Moros, Los Baños, Pontet, Falguera and Forcas (Fernández-López de Pablo and Jochim 2010). That work suggested that the abandonment episodes were not restricted to the Central Ebro basin, but a recurrent pattern of occupation gaps and reoccupation

*Correspondence: Javier Fernández-López de Pablo, as above.
E-mail: jfernandezlopez@ua.es

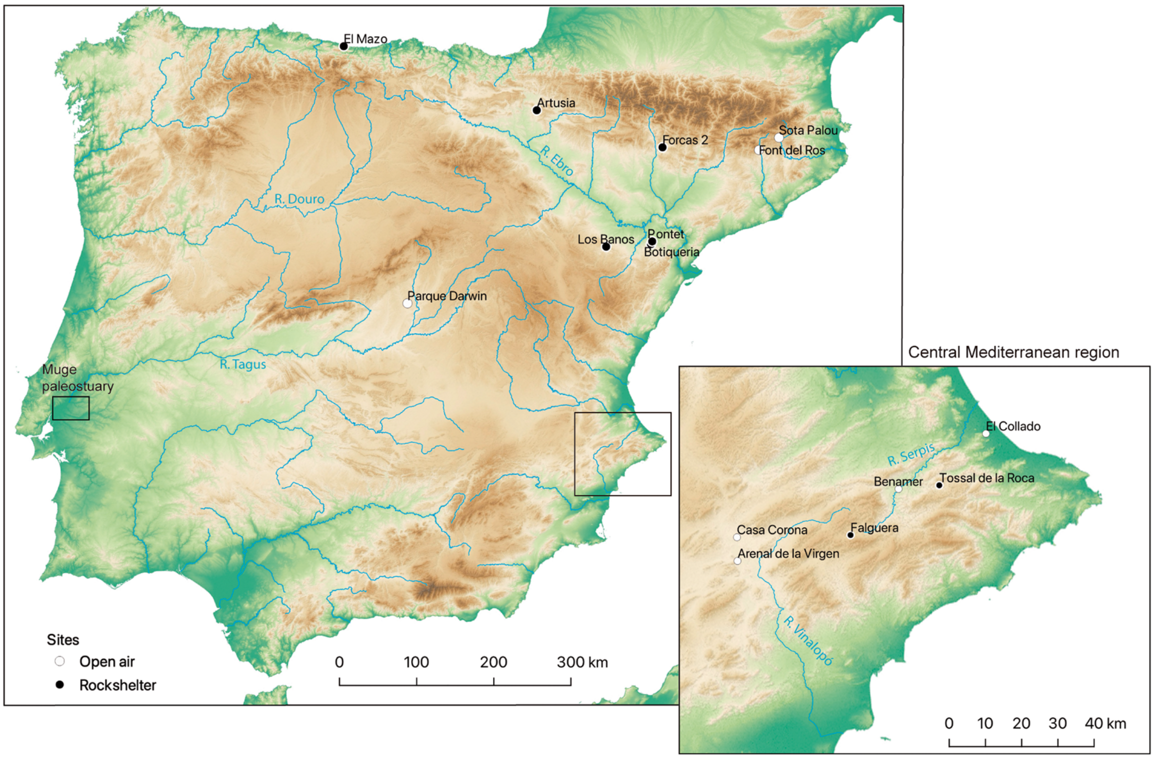

Figure 1. Left: map of the Iberian Peninsula with the location of the main archaeological sites discussed in the text. Right: detailed view of the Central Iberian Mediterranean Region where El Arenal de la Virgen site is located.

episodes, spanning the chronology of the 8.2 k cal a BP climatic event, was also documented in other archaeological sequences in the Iberian Mediterranean region. Thus, in light of the discussed chrono-stratigraphic evidence, the kind of occupation (rockshelter temporary camps) and the composition of faunal assemblages, it was proposed that these types of abandonment episodes might have been caused by adjustments in foraging logistic mobility systems during periods of climatic deterioration.

Immediately after the above papers were published, new studies from other Iberian areas discussed the impact of the 8.2k cal a BP climatic event on Mesolithic communities (Bicho *et al*., 2010; Cortés *et al*., 2012). In the central Atlantic coast of Portugal, the 8.2k cal a BP climatic event was associated with a decrease in upwelling activity, favouring the concentration of biological marine productivity in the palaeoestuary of the Muge river (Van Der Schriek *et al.,* 2008). Building on previous hypotheses connecting this shift in biological productivity with the onset of the Muge shell middens (Zilhão 2003; Martins *et al*., 2008), Bicho *et al*., (2010) demonstrated a clear chronological correlation using the extensive radiocarbon record of Mesolithic sites of central Portugal. Thus, in this area of Atlantic Europe, this climatic event triggered very significant transformations in patterns of settlement and subsistence, with semi-permanent occupation shell mounds, a more intensive exploitation of estuarine resources and the appearance of cemeteries (Bicho *et al*., 2010).

In contrast, in the southern coast of Iberia the 8.2k cal a BP climatic event was tentatively correlated to changes in thermohaline circulation and increasing upwelling variability in the Alborán sea, leading to a reduction of marine biological productivity. It has been suggested that such coastal environmental changes hampered the reliance on marine resources and favoured the abandonment of some sites during the Mesolithic period (Cortés *et al*., 2012).

More recently, different works have examined the impact of the 8.2k cal a BP climatic event on Mesolithic settlement systems using detailed stratigraphic and palaeoclimatic records on single sites (García-Martínez de Lagrán *et al*., 2016, García-Escarzaga *et al*., 2022). In the Upper Ebro Valley, the Artusia rockshelter provided stratigraphic evidence of two arid events dated to ca. 8500 cal a BP (Unit 4) and 8200 cal a BP (Unit 7), in which the tufa formation was interrupted (García-Martínez de Lagrán *et al*., 2016). The second aridity event (Unit 7) was associated with a decrease in occupation intensity inferred from the absolute frequencies of lithic and faunal remains in the stratigraphic sequence of Artusia, a pattern that has been also suggested for other Mesolithic sites of the Ebro Valley (García-Martínez de Lagrán *et al*., 2016).

In Eastern Asturias, the stratigraphic sequence of El Mazo rockshelter, a shell midden deposit, has provided new evidence regarding the palaeoenvironmental signal of the 8.2 k cal a BP climatic event on sea surface temperatures and intertidal mollusc exploitation patterns in coastal systems of northern Iberia (García-Escárzaga *et al*., 2022). Based on $\delta^{18}O$ stable isotope evidence from *Phorcus lineatus*, that study reported a 2.3 °C decrease in sea surface summer temperatures during ca. 8315–8070 cal a BP, which was correlated with increasing harvesting pressure of *Patella vulgata*, a cold-adapted species.

Finally, different regional studies used time series analyses of summed probability distributions of calibrated radiocarbon dates (SPD) to discuss the impact of the 8.2k cal a BP climatic event on Iberian Mesolithic populations (Bernabeu *et al*., 2014 and 2016; Montes *et al*., 2016; Fyfe *et al*., 2019; Alday *et al*., 2018; Fernández-López de Pablo *et al*., 2019; McLaughlin *et al*., 2021; Clark and Barton 2022). These studies reported very different results: from studies identifying positive trends in demographic growth such in the Iberian Atlantic areas of Central Portugal (McLaughlin *et al*., 2021) and Asturias–Cantabria (Clark and Barton 2022), to others that do not identify a clear impact as in the Mediterranean area (Fyfe 2019) and the Ebro valley (Clark and Barton 2022; Alday *et al*., 2018), or those that, at subregional level, have identified both positive and negative trends (Fernández-López de Pablo *et al*., 2019; Bernabeu *et al*., 2016; Montes *et al*., 2016).

In the present work, we approach the study of resilience and vulnerability of Mesolithic communities to Early Holocene environmental dynamics and ACEs using archaeological data of open air-sites in the SE Iberian Peninsula. In particular, our case study follows recent approaches focused on single sites, encompassing high-precision archaeological chronologies, coupled with detailed local palaeoclimate records (Blockley *et al*., 2018). In this work, we present the methodological design and first results of an integrated research programme that centres on new excavations at Arenal de la Virgen, a lake side site in the Upper Vinalopó Valley (Alicante, Spain). New extensive open-area excavations, multi-scalar geoarchaeological and archaeo-stratigraphic studies, together with featured-based palaeobotanical analysis, were conducted to design a specific radiocarbon programme and produce different Bayesian chronological models. The posterior probability distributions of each occupation phase were compared with the environmental dynamics inferred from the nearby palaeoecological records of the Salines Playa-lake (Burjachs *et al*., 2016) and Villena palaeolake (Jones *et al*., 2018). The latter's raw data sets were reproduced for this study using a novel Bacon age–depth model. The relevance of this integrated multiproxy archaeological and palaeoecological approach lies in the identification of the relationship between settlement dynamics and aridity patterns, during the Early to Middle Holocene transition, at local and subregional scales in one of the driest areas of the Iberian Peninsula.

Materials and methods

Site description and regional settings

El Arenal de la Virgen (38.615293 lat., −0.926753 long., 497.77 m a.s.l) is an open-air site located in the southwestern margin of the Villena palaeolake in the upper Vinalopó Valley (Fig. 2). The site is located in the Villena basin, about 80 km from the Mediterranean coast in the southeastern section of the Iberian Peninsula. The hydrology of this area is characterized by ephemeral and permanent lagoons as well as ponds fed by runoff and ground water. Previous geomorphological and sedimentological studies have shown very intensive aeolian activity in the area during the Holocene (Casquel *et al*., 1989; Jones *et al*., 2018), producing sand deposits in the form of dunes and aeolian sheets (Ferrer and Fumanal, 1997). With a mean annual temperature of 15 °C, and annual precipitation of 324 mm, with yearly peaks in autumn and spring, the contemporary climate is continental sub-arid Mediterranean. The annual water balance for the area is manifestly negative, with a mean annual potential evaporation of 750 mm. The site lies on a small glacis, covered by an aeolian sand sheet located between the foothills of the Cretacic relief of Sierra del Catellar (734 m a.s.l.) and the western bank of the Villena palaeolake. The site was discovered in the 1950s due to its surface scattering of Early Cardial Neolithic pottery sherds and lithic artefacts (Soler, 1965; Fortea 1973; Gómez-Puche and Fernández-López de Pablo 2016).

In 2006, a new research programme consisting of trial trenches and test pits was conducted in the adjacent field, allowing Early Holocene archaeological deposits to be located (Fernández-López de Pablo *et al*., 2008). Subsequent fieldwork in 2007, consisting of a 6-m^2 test pit, provided the first chrono-stratigraphic evidence of Mesolithic occupations at this site (Fernández-López de Pablo *et al*., 2011a and 2011b).

Fieldwork methods

A new phase of fieldwork was developed in 2017, following an open-area strategy which considerably expanded the excavation area from 6 to 84 m^2. The excavation followed the 2007 fieldwork grid system and datum (497.77 m a.s.l.), based on 1-m^2 excavation squares. In addition, each excavation unit was further subdivided into 0.25-m^2 sub-squares. The archaeological deposit was manually excavated according to

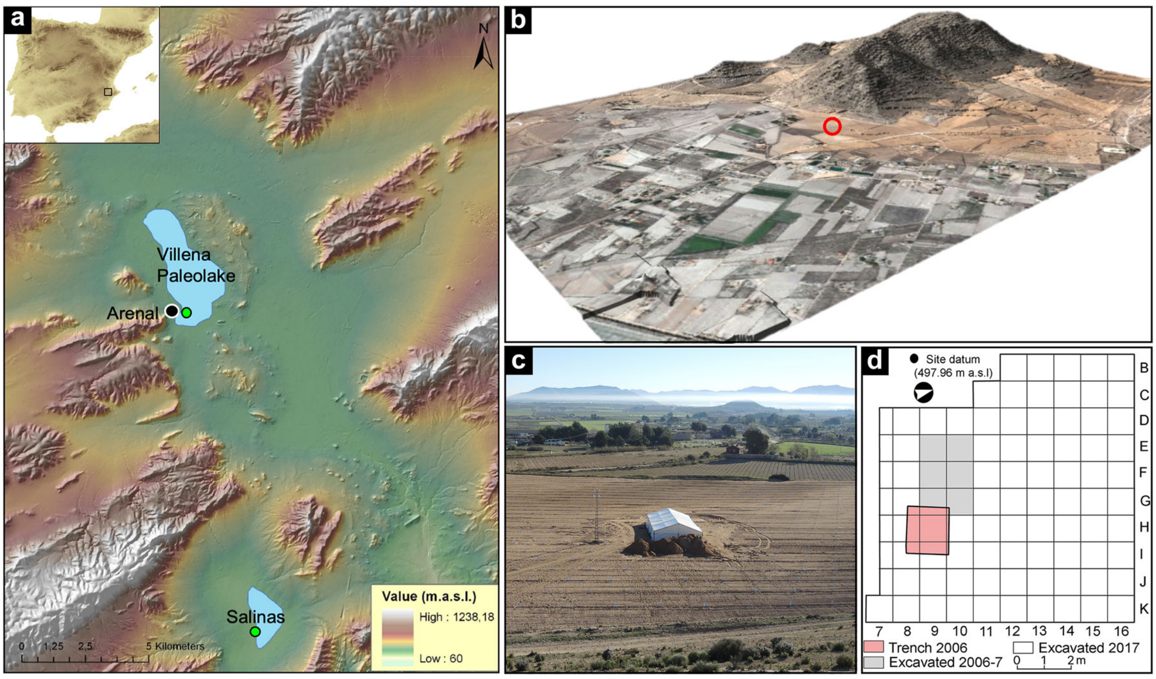

Figure 2. (a) Upper Vinalopó Valley: location of the Arenal de la Virgen site and the palaeoecological records of Villena and Salines; (b) 3D topographic reconstruction of the location of the Arenal de la Virgen site facing the Villena palaeolake (grey colour parcels) and the Sierra del Castellar; (c) general view of the site during the excavation fieldwork in 2017; (d) site plan showing the excavation units along the different fieldwork campaigns.

the dip of strata. The location of each finding was recorded three-dimensionally using the ARCH·e System Fieldwork, a wireless data recording network that integrates a robotic total station (Trimble S8) and fieldwork PDAs with a server containing the central data repository (Canals *et al.*, 2008; Canals and Guerra 2011). The sediment was dry sieved through a 5- and 2-mm mesh on site. A selection of sediment samples together with the fill of occupation features were wet sieved (through the same mesh) and floated for recovery of macro-botanical remains. For every sieve and flotation find, random *x–y–z* coordinates were generated within 0.0125 m^3 (0.05 × 0.05 × 0.05 m).

During the excavation, the sedimentary units and archaeological features were independently recorded as numbered Strata and Stratigraphic Units (SUs) using the Harris system (Harris 1989), on the basis of the sediment's macroscopic properties (changes in colour, texture and consistency). For each SU, the excavation process was documented by digital photography and the morphometric dimensions recorded by photogrammetry, using mosaics of overlapped digital photographs georeferenced to the excavation grid with PhotoScan.

Micromorphology, soil chemistry and textural analysis

Intra-site sedimentary contexts were investigated using micromorphology, soil chemistry and textural analysis of both sedimentary strata (analysis of excavation profiles) and archaeological features. During the excavation, field descriptions and systematic sampling of unearthed surfaces and profiles were conducted at the site. For the purposes of the work presented here, a aystematic study of the stratigraphic profile E was conducted. Twenty thin sections from block sediment samples were analysed for micromorphology, and 38 bulk samples for soil chemistry (carbonate content, organic matter, pH) and texture. Both block and bulk samples were collected from the same spots and they document vertical and lateral changes of the stratigraphic sequence. Results obtained from the analysis of the archqeological features are dealt with in detail elsewhere (Polo-Díaz *et al.*, 2022).

Radiocarbon dating

A radiocarbon dating programme was specifically designed to disentangle the occupational palimpsest and to estimate the duration of each phase. One of the main challenges affecting the radiocarbon sampling strategy of the Arenal de la Virgen site was the null preservation of bone, presumably due to sediment taphonomy and post-depositional processes, and the lack of charred seeds with the minimum necessary weight for accelerator mass spectrometry (AMS) radiocarbon dating.

In addition, open-air sites associated with aeolian deposits, such as Arenal de la Virgen, are very often subject to bioturbation, pedogenic and deflation processes (Crombé 2015, Zilhão 1998), which can potentially affect the spatial and stratigraphic association between radiocarbon samples and human activity (Crombé *et al.*, 2013). To avoid stratigraphic association problems, we selected charcoal samples retrieved from clearly anthropogenic sedimentary facies associated with archaeological structures within the sedimentary strata III and IV. The archaeological structures sampled generally correspond to fire-related features (SU608, SU611, SU612, SU613, SU615, SU620 and SU623) and dwelling structures (SU604 and SU628). Finally, we also selected two charcoal samples from the upper part of Unit IV (SU607) which overlays the archaeological features of the site's northern sector (SSUU608 and 611).

The radiocarbon samples correspond to single charcoal fragments, taxonomically identified according to genus or species. The high degree of fragmentation prevented us from determining whether the charcoal samples were part of small twigs or of outer tree rings (Pettit *et al.*, 2003). They were, therefore, subject to a certain degree of chronological uncertainty. In contrast, two samples of pinecone scales, retrieved in SU604 and 613, provided short-life inbuilt radiocarbon ages. Considering this, to evaluate the stratigraphic consistency of the radiocarbon dates and the potential chronological offset derived from the old wood effect (Schiffer, 1987) on a feature basis, we dated more than one sample from features SU608, 613, 615 and 604. The ^{14}C AMS radiocarbon dating was conducted at the Beta Analytic laboratory, using their standard pre-treatment techniques for charcoal samples, applying the acid–alkali–acid (AAA) method. Calibration was performed with OxCal 4.4 (Bronk Ramsey, 2017) using the IntCal20 atmospheric curve (Reimer *et al.*, 2020).

Lithic analysis

For morpho-technical analysis of the lithic assemblage from Arenal de la Virgen, each lithic remain was classified into a structural category according to its position inside the production chain (Carbonell *et al.*, 1992) and the technical attributes of each were also described (Andrefsky 2005; Inizan *et al.*, 1999). Knapping methods were defined based on the description of cores, by means of faciality, on the arrangement of the removals and morphology of the negatives, complemented with the technical attributes identified for the knapping products. For concordance with the regional setting, the typological classification of the retouched elements followed Fortea's typology, established for the Epipalaeolithic of the Iberian Peninsula's Mediterranean region (Fortea, 1973).

Archaeobotanical analysis

About 2025 litres of archaeological sediments were processed with a flotation machine to recover macro-botanical remains. In addition to the sieving conducted during flotation, 1- and 0.25-mm meshes were used to retrieve small remains and to minimize the fragmentation of the material, using a similar processing technique to that successfully applied on other archaeological sites (Martínez-Varea, 2016; Vidal-Matutano *et al.*, 2015). After drying, samples were additionally sieved through a column of 4-, 2-, 1-, 0.5- and 0.25-mm meshes. The obtained fractions of each flotation sample were subsequently sorted using a binocular microscope (Leica M165C) at the Laboratory of Prehistory and Archaeology Milagro Gil-Mascarell of the Universitat de València. Charcoal and seed analyses were also carried out. Charcoal analysis is based on the botanical identification of carbonized wood, i.e. determining which species the charcoal is derived from. Each fragment was observed under reflected light brightfield/darkfield optical microscopy with a set of lenses ranging from 50× to 1000× magnifications. Wood anatomical features were compared with those provided by specialized literature on plant anatomy (Schweingruber, 1990) and a reference collection of modern charred wood.

For the standard analysis, charcoal was broken manually and without using chemical additives so the samples could be used for radiocarbon dating (Vernet *et al.*, 1979). To observe specific features and record images, we used a Hitachi S-4100 scanning electron microscope available at the Central Service for Experimental Research Support (SCSIE) at the Universitat de València.

The frequency of the taxa identified was measured as a percentage of fragment counts when the sample contained a statistically meaningful number of charcoals, depending on the taxonomic diversity (Chabal, 1988; Chabal *et al.*, 1999). The identified taxa, in addition to the human selection of plant resources available, reflect part of the woody vegetation that was exploited and that was thus present among the local flora (Chabal, 1997). Therefore, charcoal analysis can be considered a reliable tool for palaeoeconomical and palaeoenvironmental reconstruction.

The seeds were identified according to metric and morphological criteria, by comparing them with the reference collection available at the aforementioned laboratory, and by using a specialized bibliography (Bojňanský and Fargašová, 2007; Cappers *et al.*, 2009).

Off-site pollen analyses and Bayesian age–depth modelling

Two lake records near Arenal de la Virgen, the Villena palaeolake and Salines playa-lake, recently published in Jones *et al.* (2018) and Burjachs *et al.* (2016), provide multi-proxy evidence of the palaeoecological and palaeohydrological dynamics during the site's human occupations. The Villena palaeolake core is located 1.47 km NE of the Arenal de la Virgen site. This record provides a 9.3-m-deep sedimentary succession, spanning Marine Isotope Stage 3 (MIS3) and the Early and Middle Holocene (Jones *et al.*, 2018). High-resolution pollen, geochemical and mineralogical data are available from the Early Holocene to the Middle–Late Holocene transition framed by a Bayesian age–depth model. They reveal a series of aridity events, including a prolonged period of aridity spanning the 8.2k cal a BP climatic event (Jones *et al.*, 2018). The Salines playa-lake is slightly further afield and is located 10 km south of the Arenal site. It presents a stratigraphic succession covering GI-1, GS-1 and the Early Holocene with pollen (Julià *et al.*, 1994, Burjachs *et al.*, 2016), mineralogical data (Giralt *et al.*, 1999) and ostracod data (Roca and Julià 1997). More recently, Burjachs *et al.* (2016) integrated the previous pollen, mineralogical, micro-charcoal and ostracod evidence into a new Bayesian age–depth model, adding new pollen-based indexes of aridity.

For the purposes of this work, improve the chronological resolution of the palaeoecological dynamics, we produced a new Bayesian age–depth (Supporting Information, section 4) model using 'Bacon' (Blaauw and Christen, 2011) for the Villena Paleolake.

The raw pollen counts of Villena and Salines (Jones *et al.*, 2018; Burjachs *et al.*, 2016) were used to produce two new pollen diagrams for the chronological interval spanning Arenal de la Virgen's human occupations. For Villena, the new pollen diagram was produced according to a new Bacon age–depth model (see below), covering the vegetation dynamics between 7400 and 9100 cal a BP. For Salines, the pollen diagram represents the vegetation patterns between 7800 and 9600 cal a BP. In addition, the pollen data from Salines playa-lake were used to produce two pollen-based curves reflecting precipitation (according to Fletcher *et al.*, 2010) and aridity (Burjachs *et al.*, 2016).

Results

Stratigraphy

Five strata were identified in the sedimentary deposit. They are named, from bottom to top, Units V, IV, III, II and I, based on field descriptions, texture, soil chemistry and micromorphological descriptions (see Figs. 3 and 4).

Unit V

A continuous deposit, 90 cm thick at its deepest point, although the base of the accumulation was not reached during the excavation process. This accumulation is fine-grained, consisting mainly of subangular quartz grains with a bimodal pattern dominated by fine and medium sands. Very scarce subangular gravels and clasts of up to 10 cm were randomly documented. Calcium carbonate concentration is relatively high while the organic matter content is low and represented mainly by sand- and silt-sized fragments of charcoal that are randomly distributed. Iron–manganese features in the form of stainings and nodules indicative of temporal waterlogged conditions were frequently observed in the matrix. No clear internal microstratification was observed in this unit.

Unit IV

This unit presents 40 cm of maximum thickness, and is documented in most of the excavation surface except for the western section, where it was not observed. This is probably due to the impact of erosive processes (deflation and surface dynamics) involved in the accumulation of units III and II. Such processes were also involved in the erosion of the top section of the Unit IV in the NE sector. Consisting mainly of fine sediments, the deposit also includes randomly distributed limestone gravels, stones and boulders up to 10 cm long. Shallow pockets filled with dark sediment (archaeological SU604) of variable morphologies and dimensions are characteristic of this Unit (see 'Archaeology: occupation features' below). The formation processes of these dark features in their sedimentary context are currently the subject of a separate detailed geoarchaeological study. Textural patterns, pH and mineral composition of Unit IV were comparable to those observed in Unit V. The concentration of organic matter was very similar in all samples from Unit IV (0.11–0.16%), except in the area corresponding to SU604, where much higher values (1–1.08%) were observed (Polo-Díaz *et al.*, 2022). The carbonate concentration was notable, the highest values reaching 10–16%. Such concentration of carbonates is directly linked to the development of calcitic features of pedogenic origin formed *in situ* as observed in thin section. Micromorphological analysis of the dark pockets of sediment (SU604) also showed frequent bioturbation features related to soil fauna and plant growth. The latter points to a discontinuity in sediment accretion and stable surface conditions during the formation of Unit IV. A sedimentary discordance related to the intensification of soil fauna activity detected at different points of the deposits marks the boundary between strata IV and III (Supporting Information-section 1, Fig. S1).

The intense carbonate redistribution suggested conditions of relatively high humidity, supported by a concentration of iron–manganese features formed *in situ* (favoured also by accumulated decomposing organic matter) and the presence of vughs in the matrix. The two latter features are probably indicative of short periods of water saturation affecting the deposit, possibly from water table fluctuations and/or occasional sedimentary surface events.

Unit III

This is also a massive accumulation, 20–25 cm thick, with a NW–SE dip. This deposit is documented in most of the excavation surface, although it narrows progressively towards

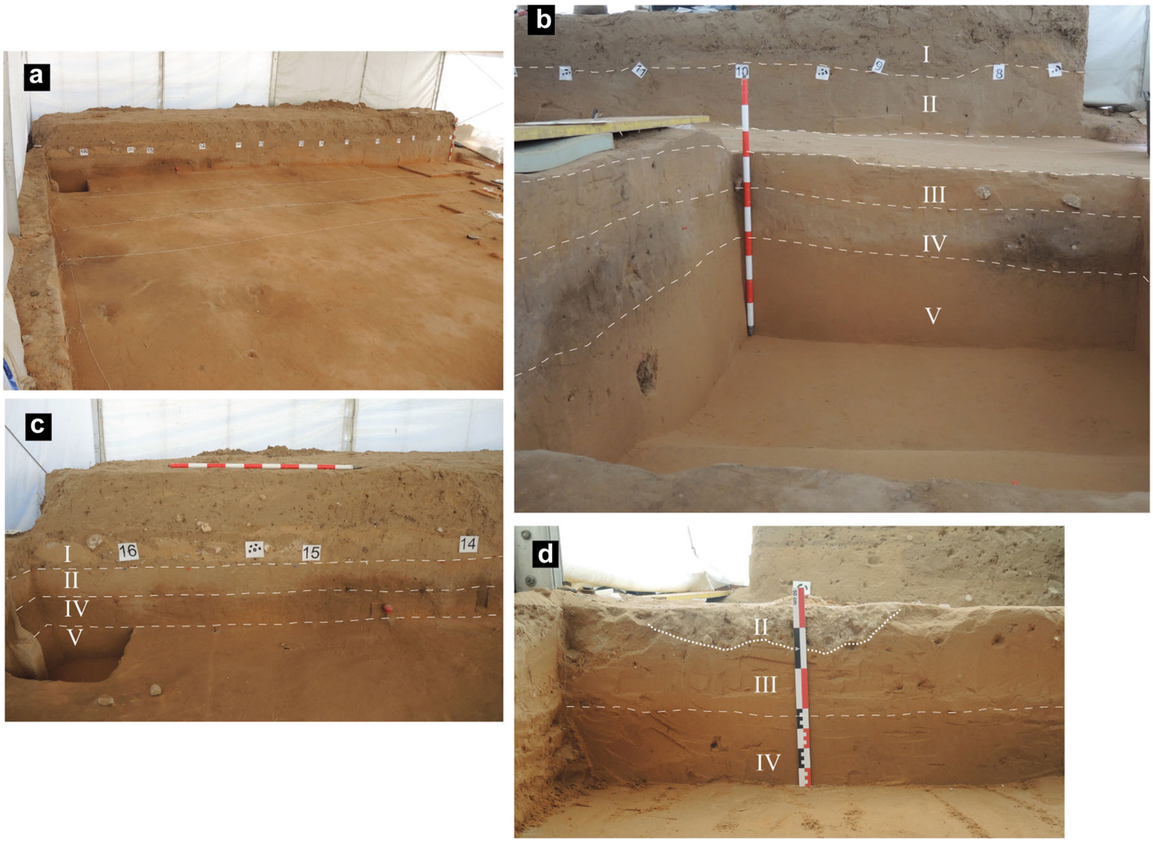

Figure 3. Stratigraphic sequence of El Arenal de la Virgen. (a) View of the excavation area from the NE showing the entire extension of the East section. (b) Detail of the southern end of the East section, indicating the strata documented in the profile, from bottom to top: Units V, IV, III, II and I. (c) Detail of the northern end of the East section. Note the lateral variability with respect to the southern end of the profile involving abrupt contact between Units II and IV as a result of erosion of Unit III and the upper portion of Unit IV. (d) Detail of the southern end of the West section. Note the run off channel containing a coarse fraction (delimited by discontinuous line) in Unit II eroding Unit III.

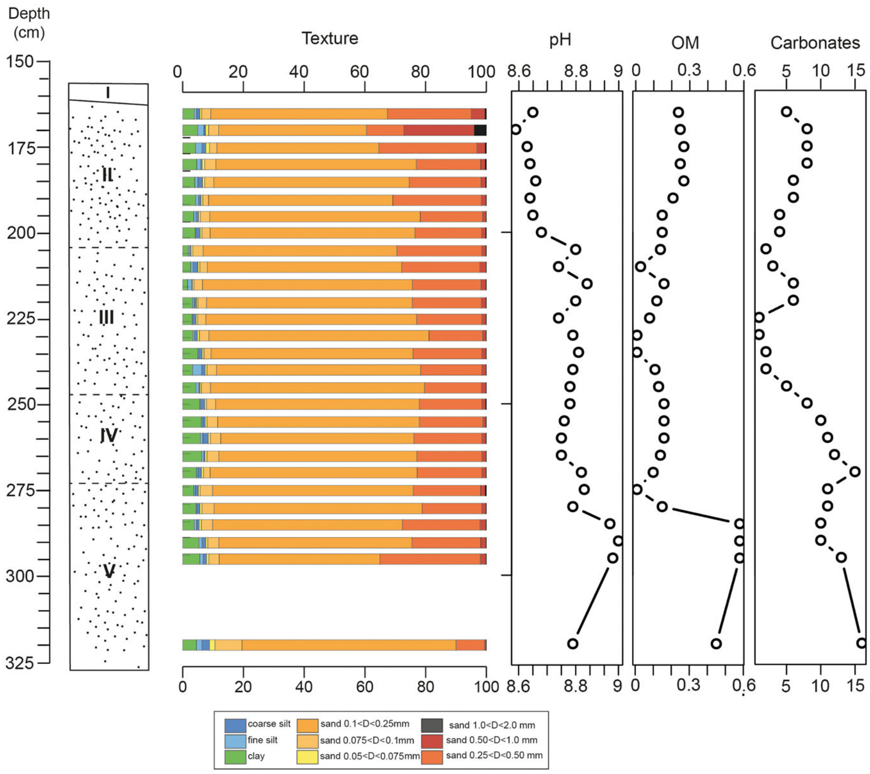

Figure 4. Stratigraphic sequence of Arenal de la Virgen, corresponding to the Eastern stratigraphic section with the associated fraction, carbonates, organic matter and pH values (see Supplementary Information Table 1).

the centre of the excavated area to disappear in the NE sector, where only isolated patches of the unit are preserved. As in the case of the underlying strata, the sediment is predominantly fine-grained, with dispersed, embedded, limestone gravels, stones and boulders with a subangular morphology.

Significantly low calcium carbonate concentrations (<3–6%) were shown by soil chemistry and supported by decarbonation features observed via thin-section analysis. Clay concentration was also significantly lower in Unit III with respect to strata V and IV, which correlates with calcium carbonate values and decreased biological activity. This evidence, in addition to the predominance of fine-medium quartz sands in the textural pattern, allows us to infer an environmental shift towards aridification linked to aeolian dynamics with a relatively high capacity for sediment classification.

Unit II

This is a massive accumulation documented in most of the excavation surface. The deposit shows a NE–SW dip, with a minimum and maximum thickness of 17 and 47 cm in the NE and SW sectors, respectively. It also presents erosive upper and lower boundaries which were clearly detected locally. Limestone gravels and boulders of up to 10 cm were found. They were generally dispersed, although in the S and W sectors of the excavation area, they were found to form concentrations and palaeochannels (Fig. 3d). Possible mixtures of strata II and III were detected locally in the NE and S sectors.

Micromorphological and soil chemistry data from the analysis of sediments of the E sector of Unit II showed a greater concentration of the coarse fraction linked to colluvial processes from splash, together with a significantly higher calcium carbonate content despite considerable lateral variability (12–13% in the NE area and 4–8% in the SE area). Correlation of this evidence with field observations mentioned above highlights the role of surface dynamics, linked to increased environmental humidity in the formation of Unit II.

Unit I

This is a continuous, 30–60-cm-thick accumulation related to modern levelling and ploughing.

Archaeology: occupation features

Enlargement of the excavation area has significantly increased the amount of occupational evidence documented on the site compared to the 2007 excavations. Figure 5a shows the spatial distribution of the archaeological features along the three occupation phases documented in the Arenal de la Virgen sequence. These archaeological features are subject to a more detailed geoarchaeological analysis elsewhere (Polo-Díaz *et al.*, 2022). Here, we present a summary description of the different archaeological features associated with each phase, relying on morpho-metric characteristics, archaeological components, radiocarbon dates and some relevant micromorphological data.

Below, we present the different features of each archaeological phase.

Phase 1

Two archaeological features (SU608 and 611) were identified in the northern area of the excavation surface, both stratigraphically associated with Unit IV. SU608 (Fig. 6a) shows an irregular ellipsoid shape, with maximum dimensions of 0.6 m in length, 0.4 m in width and 0.2 m in depth. A concentration of limestone clasts was recorded at the bottom of this structure, whose sedimentary infill contained a modest density of macro-botanical remains (1.78/litre) and lithic artefacts. Two charcoal samples retrieved from the bottom (8220 ± 30 BP, Beta-493220) and the upper part (7700 ± 30 BP, Beta-493219) of the sedimentary infill yielded statistically different radiocarbon dates, suggesting the intrusive character of the upper part (Beta-493219), considering its similarity to the radiocarbon ages provided by samples of phase 2 (see below).

SU611 (Fig. 6b) presents very similar morphology and dimensions to SU608. This shallow pit, located 1.5 m from SU608, also displays an ellipsoid plan with maximum length of 0.6 m, width of 0.4 m and depth of 0.2 m. The dark grey/blackish sediment infill of this structure contains a significant concentration of *Quercus* charcoals (25.95/litre), lacking any other sort of archaeological components (e.g. lithic artefacts, limestone clasts). An evergreen *Quercus* sp. charcoal was radiocarbon dated to 8200 ± 30 BP (Beta-473942), providing a statistically similar radiocarbon age to that of SU608.

Phase 2

Phase 2 encompasses six archaeological structures: SSUU604, 628, 615, 613 612 and 623, showing considerable variability in morpho-metric attributes and spatial distribution between them and with respect to Phase 1. These structures are all associated with Unit IV, while displaying distinct stratigraphic relationships to Unit III. While it was possible to clearly establish the overlying position of Unit III with respect to SSUU604, 628, 612 and 623, this was not the case for SSUU615 and 613, due to the impact of slope processes and the partial erosion of Unit IV in the NE area of the site.

SU604 (Fig. 7a) was uncovered in 2006 and partially excavated in 2007, when it was interpreted as a hearth-pit (Fernández-López de Pablo *et al.*, 2011a). In 2017, the extension of the excavated area allowed this feature to be fully documented. It consisted of a shallow pit with an irregular subcircular shape, and a maximum length of 3 m, a maximum width of 2.35 m and a maximum depth of 0.25 m (Fig. 7c), covering a surface of 5 m^2. The sediment had a massive structure, a dark grey–brown colour and contained a variety of archaeological components as recorded in the field: angular limestone clasts, land snails, lithic artefacts, some of them with clear thermal alterations, palaeobotanical remains and ochre fragments. Both the shape and size of this feature resemble the 'type B' pits recently identified at other Mesolithic sites, which were also located in coversand areas (Peeters and Niekus., 2017; Crombé and Langhor, 2020). Micromorphology and soil chemistry data from SU604 indicated a notable increase in organic matter and of biological processes (e.g. plant growth and soil fauna activity), consistent with stable environmental conditions, favourable to the formation of this structure, in parallel to its human occupation.

In the north-eastern section of SU604, a smaller (0.32 m long, 0.18 m wide and 0.25 m deep) pit-structure was located (SU625), containing a 0.40-m-long limestone block in a vertical position (Fig. 7b). This could be interpreted as a structural feature, possibly a wedge. The spatial and stratigraphic association of both structures resembled other examples of dwelling structures documented in European Mesolithic contexts (Hernek, 2003; Verjux, 2003; Waddington *et al.*, 2003).

Two radiocarbon dates were available for SU604: the first one 7750 ± 40 BP (Beta-243772), from a wood charcoal of a

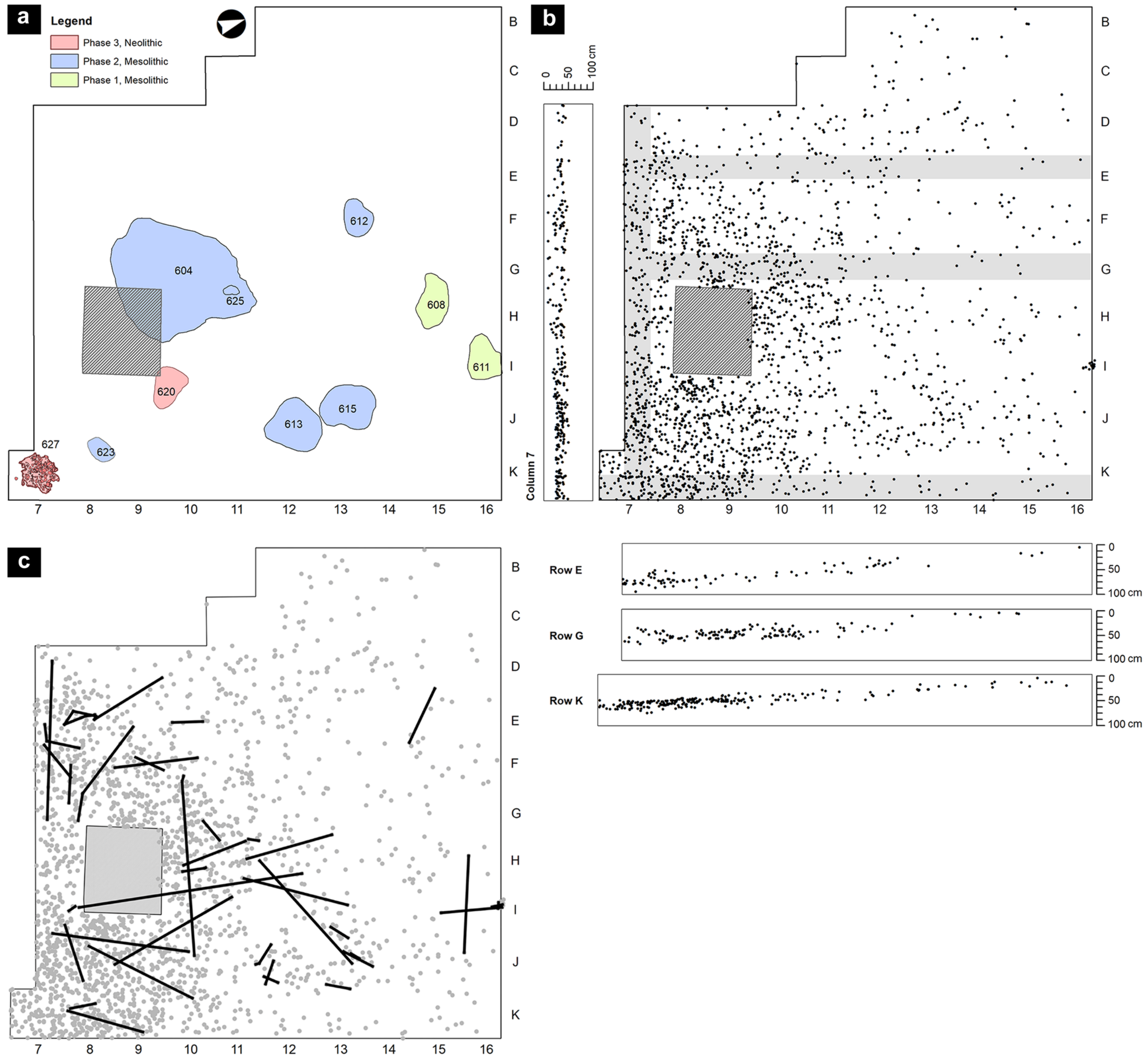

Figure 5. Occupational evidence from El Arenal de la Virgin site. (a) Composite accumulative plan with the archaeological features associated with each phase. (b) Spatial distribution and vertical archaeo-stratigraphic projections of the lithic materials. (c) Lithic connections (refits, conjoins and thermal conjoins) documented in the archaeological horizon. The grey-shaded square indicates the test-pit excavated in 2006.

Quercus sp, evergreen, and the second one 7550 ± 30 BP (Beta-493226) from a carbonized *Pinus* sp. cone. One radiocarbon age of SU625, 7850 ± 30 BP (Beta-473944) was also obtained from a *Quercus* sp. *evergreen* charcoal. The time interval provided by SU625 and 604 showed a high degree of chronological consistency, suggesting a single (and short) occupation phase, considering the inbuilt age resolution of the charcoal samples (Supporting Information, Fig. S3).

Three combustion features, SSUU613, 615 (Fig. 6d,e) and 623, equally presenting a generic subcircular morphology and containing limestone clasts were also chronologically associated with phase 2. These three features contained variable concentrations of charcoal (613 = 0.52/L, 615 = 0.73/L and 623 = 1.22/L), which were, however, higher than that recorded for Unit IV (0.03–0.16/L).

In the NE part of the excavation surface, SU613 presents maximum dimensions of 1.17 m in length, 1.08 m in width and 0.17 m in depth, whereas SU615 is a maximum 1.16 m long, 0.92 m wide and 0.25 m deep. In the southern area of the excavation, SU623 (Fig. 7d) has maximum dimensions of 0.6 m in length, 0.38 m in width and 0.12 m in depth.

The radiocarbon record again shows a high degree of chronological consistency among the dates yielded by these three structures, although some differences were observed between the pine and oak charcoal samples. SU615 was radiocarbon dated to 7470 ± 30 BP (Beta-493224) from a charcoal fragment of conifer, whilst SU623 produced a radiocarbon age on a *Quercus* sp. charcoal fragment of 7750 ± 30 BP (Beta-493223). Three radiocarbon ages were obtained from SU613, two from *Quercus* charcoals – 7820 ± 30 BP (Beta-493221) and 7770 ± 30 BP (Beta-493225) – and one from a pinecone scale – 7660 ± 30 BP (Beta-493222). The pinecone scale sample presented an age difference of 22–245 years (Supporting Information, Fig. S3) compared to the two oak charcoal samples in this structure. The oak charcoals may have been influenced by the chronological uncertainty associated with the old wood effect.

Finally, SU612 (Fig. 5c) is a shallow pit measuring a maximum of 0.77 m in length, 0.59 m in width and 0.24 m in

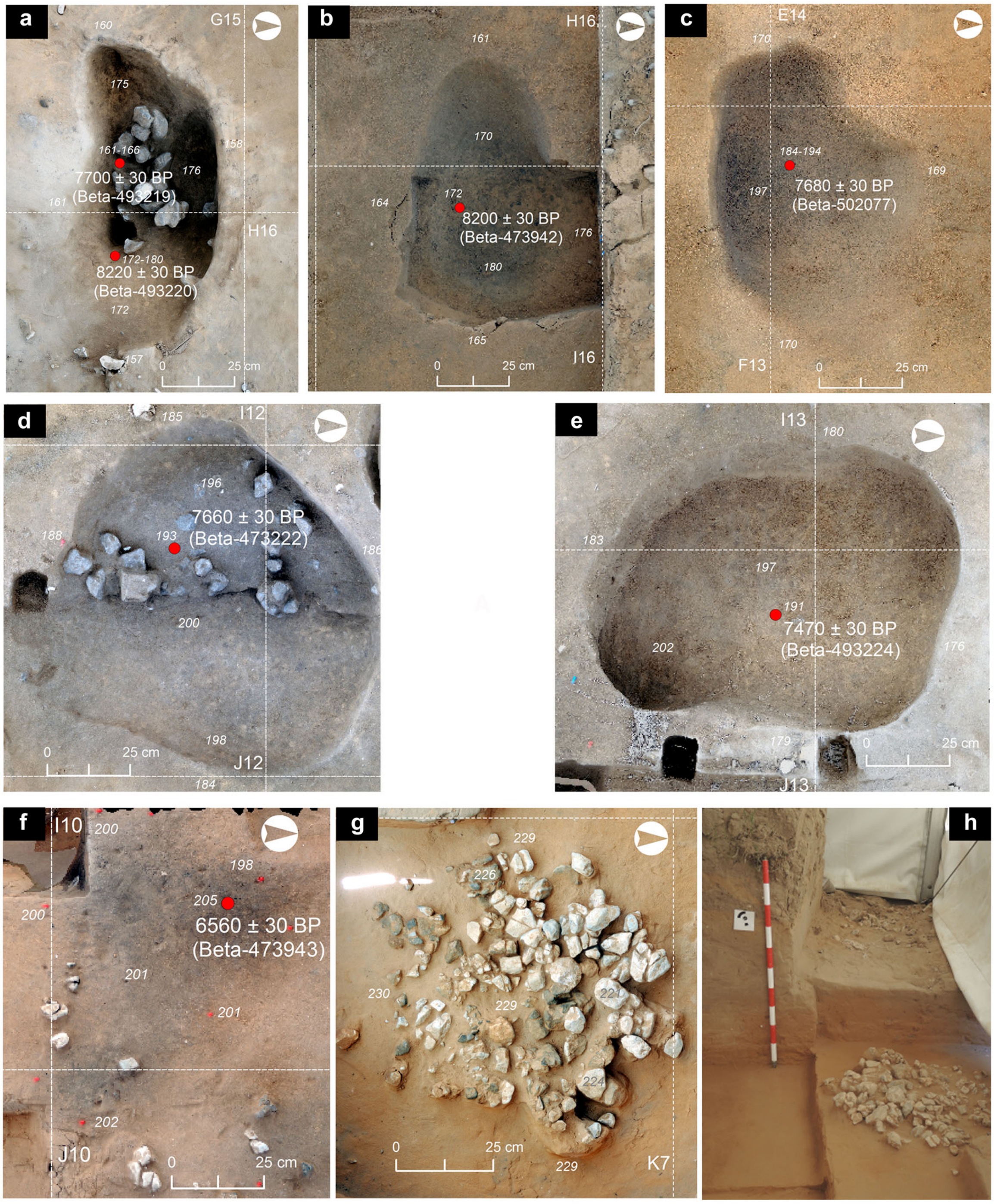

Figure 6. Arenal de la Virgen. Archaeological features. (a, b) Unit IV Phase 1 (Early Mesolithic); (c–e) Unit IV Phase 2 (Early Mesolithic); (f–h) Unit III Phase 3 (Neolithic). a. SU608; b. SU611; c. SU612; d. SU613; e. SU615; f. SU620; g, h. SU627 (orthophotography and detail of its stratigraphic position within Unit III). The red dots indicate the location of the ^{14}C samples. Elevations (in italics) are in centimetres below the datum.

depth. This structure, unlike the SUs of phase 2 presented above, lacks any other diagnostic archaeological components, such as clasts and lithic artefacts. Its palaeobotanical record shows a high density of macro-botanical remains of 1.22/L. An oak charcoal from this feature was ^{14}C dated to 7680 ± 30 BP (Beta-502077).

Phase 3

Two archaeological features were stratigraphically associated with Unit III located in the south-eastern sector of the excavation area: the shallow pit SU620 (Fig. 6f), which measures a maximum of 0.87 m long, 0.64 m wide and 0.26 m deep, was radiocarbon dated to 6560 ± 30 BP (7555–7425 cal a BP) using a charcoal sample of *Quercus* sp. evergreen. SU627 (Fig. 6g), unlike the rest of the archaeological structures presented, is a circular pavement area with maximum dimensions of 0.84 m in length and 0.71 m in width, built of intricate angular clasts. No radiocarbon dates were available for this structure given the scarcity and small size of the charcoals recovered. However, the stratigraphic position of SU627 (Fig. 6h), in the upper part of Unit III, indicated a *post-quem* chronology with respect to SU620 during the Neolithic period. Such a chrono-cultural attribution is consistent with other similar circular pavements documented in the region (García Atiénzar *et al.*, 2006; Torregrosa *et al.*, 2011).

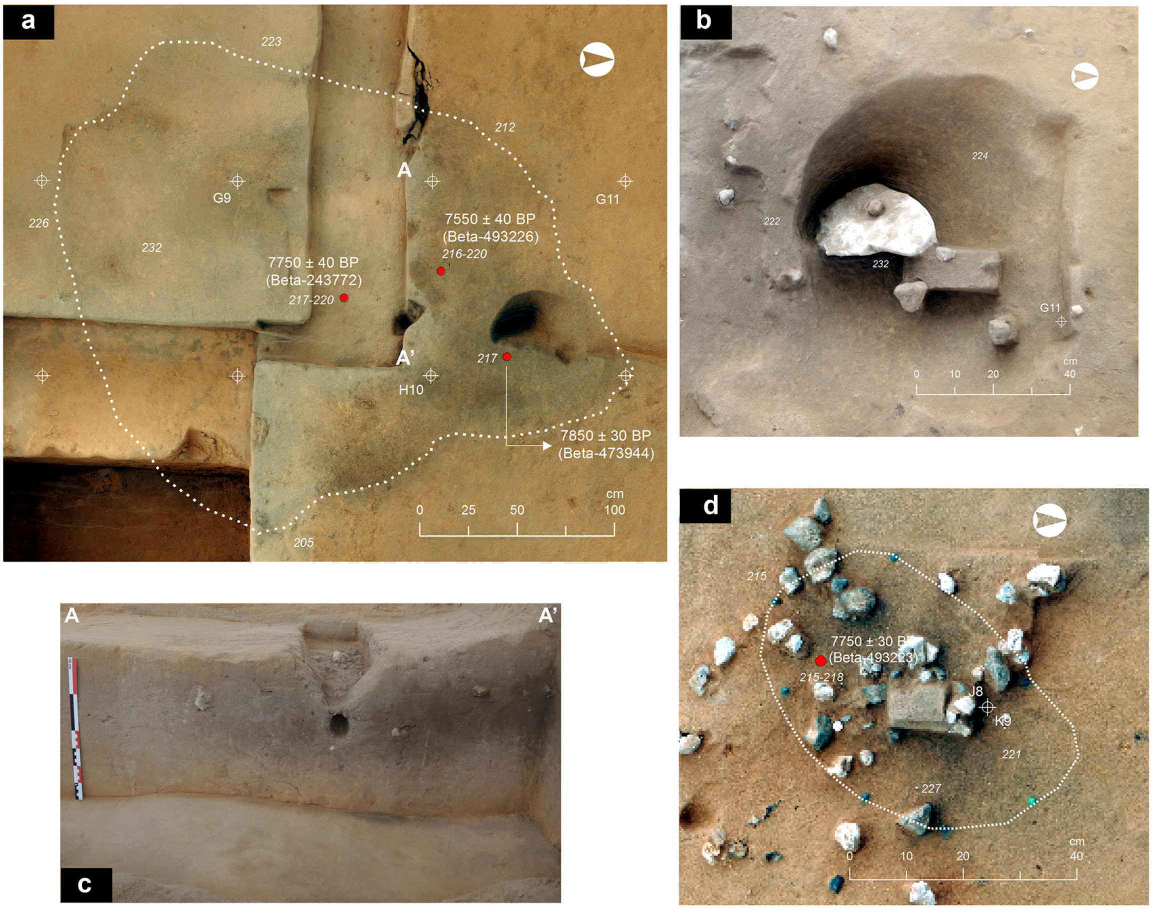

Figure 7. Arenal de la Virgen. Archaeological features: a. SU604 (orthophotography); b. SU625 during the excavation process – note the vertical position of the limestone block; c. SU604 cross-section A–A'; d. SU623. The red dots indicate the location of the ^{14}C samples. Elevations (in italics) are in centimetres below the datum.

Archaeology: radiocarbon dating and Bayesian chronological modelling

Two different Bayesian chronological models – model 1 and model 2 – were elaborated to stratigraphically constrain the posterior probability distributions of the calibrated radiocarbon ages and to estimate the duration of each chronological phase (Table 1; Buck *et al.*, 1996; Dye and Buck, 2015). Considering the stratigraphic information, we decided to use a conservative three-phase model, sequentially arranging its phases (two phases in Unit IV and one phase in Unit III), and assuming a random deposition of the dated events within each phase (Bronk Ramsey, 2009). The prior phasing of the radiocarbon record is also reported in Table 2 (and in Supporting Information, Fig. S3 where further details are provided regarding the lateral changes of the site's stratigraphy). In addition, we used the *Span*() and *Interval*() functions in Oxcal (Bronk Ramsey, 2009), to probabilistically establish the duration of each occupation phase and the chronological hiatuses between phases. The calibration of individual dates as modelled distributions is also reported in Table 1 and Fig. 8.

Model 1 is based on the whole radiocarbon record, 15 dates, showing a robust agreement index [*Amodel* = 153] (Table 2). In Phase 1, the oldest occupation phase is composed of features SU608 and 611. This phase is dated to 9247–9041 cal a BP (considering the median of the modelled chronological boundaries of Unit IV–Phase 1). Both features showed statistically similar radiocarbon ages, indicating a short occupation span (0–168 years) for this phase at 95.4% confidence interval (CI). Phase 1 was culturally assigned to the Early Mesolithic of Notched and Denticulates.

The *interval* () function estimates a chronological hiatus between phases 1 and 2 of 68–625 years (95.4% CI). This second occupation phase is well dated at the site, with 12 radiocarbon dates from different combustion structures, one domestic structure and two samples from the uppermost section of Unit IV. The chronological range of Phase 2, according to the medians of the modelled boundaries of Level IV–Phase 2, was dated to 8630–8292 cal a BP. The Phase 2 timespan was estimated to be 218–397 years (95.4% CI) and might reflect the recurrent use of this space over successive occupation episodes. Such an estimation, however, could have been influenced by the old wood effect problem (Pettit *et al.*, 2003). To estimate the chronological uncertainty within this phase, we decided to conduct pairwise comparisons between radiocarbon ages of evergreen *Quercus* charcoal and pinecone scale samples from features SU604 and SU613. To do this, we assumed that pinecone scales have inbuilt ages similar to short-lived samples. Using the *Difference*() function in Oxcal, we estimated a potential old wood effect offset of 38–265 years for SU604 and 29–232 years for SU613, obtaining, in both cases, a 95.4% CI (Supporting Information 1, Fig. S3). This analysis showed that both features might be affected by a similar degree of chronological offset due to the old wood effect. Considering this, we decided to improve the chronological resolution in Phase 2 by producing a second Bayesian Phase model (model 2) with the same structure and prior information as model 1 but using only the radiocarbon dates on pinecone scales for Phase 2. Under the premises of model 2 (Tables 2 and 3), the chronological boundaries

Table 1. Radiocarbon record and calibrated ^{14}C radiocarbon dates (unmodelled posterior distributions) from El Arenal de la Virgen archaeological sequence.

Unit	Phase	Stratigraphic Unit/spit	Z	Sample	Lab. ref	^{14}C BP age	^{13}C	Age (cal a BP)
IV	1	608/3	180–172	*Quercus* sp. evergreen	Beta-493220	8220 ± 30	−27.9	9394–9027
IV	2	608/1	166–161	*Quercus* sp. ever-green	Beta-493219	7700 ± 30	−23.7	8547–8411
IV	1	611	170	*Quercus*sp. evergreen	Beta-473942	8200 ± 30	−26.4	9275–9026
IV	2	625	217	*Quercus*sp. evergreen	Beta-473944	7850 ± 30	−25.5	8765–8546
IV	2	613/1	184–187	*Quercus*sp.ever-green	Beta-493221	7820 ± 30	−25.4	8698–8520
IV	2	613/1	194–190	*Quercus* sp. evergreen	Beta-493225	7770 ± 30	−25.8	8600–8449
IV	2	613/2	193–187	*Pinus* cone scale	Beta-493222	7660 ± 30	−28.1	8536–8389
IV	2	623/1	215	*Quercus* sp. evergreen	Beta-493223	7750 ± 30	−26.6	8594–8430
IV	2	604	217	*Quercus*sp. ever-green	Beta-243772	7750 ± 40	−25.8	8595–8426
IV	2	604/4	220–216	*Pinus* cone scale	Beta-493226	7550 ± 40	–	8420–8210
IV	2	612	187–194	*Quercus* sp. evergreen	Beta-502077	7680 ± 30	−26.6	8541–8407
IV	2	615	191	Conifer	Beta-493224	7480 ± 30	–	8371–8195
IV	2	Level 4/top2	180–172	*Quercus*sp. ever-green	Beta-493228	7790 ± 30	−25.8	8636–8458
IV	2	Level 4/top1	171–168	Conifer	Beta-493227	7470 ± 30	−23.2	8365–8193
III	3	620	205	*Quercus*sp. evergreen	Beta-473943	6560 ± 30	−26.0	7560–7425

estimated for Phase 2 were 8430–8268 cal a BP, with a span of 0–180 years (95.4% CI), i.e. a significantly shorter one than that of model 1.

Phase 3 (Unit III) was composed of a single radiocarbon age, Beta-473943, of Early Neolithic chronology. Both models highlighted a chronological hiatus between phases 2 and 3, which was associated with the beginning of the deposition of Unit III under very arid conditions.

In summary, the Arenal de la Virgen radiocarbon record's three-phase Bayesian chronological model revealed two stratigraphically constrained Mesolithic occupation phases (Table 3). Cultural radiocarbon activity ceased after the end of Phase 2, which coincides with the beginning of the deposition of Unit III during the 8.2k cal a BP event, under arid conditions. Within Unit III, a third occupation phase was identified during the Neolithic period, after 7.5k cal a BP.

Palaeobotanical evidence

Palaeobotanical remains were generally very scarce, despite the intensive sampling efforts made. This is a general trend in open-air deposits with these characteristics. In terms of density of remains by volume (in litres) in bulk samples, significant differences between concentrations documented inside and outside the archaeological features (SU) were found: Unit IV produced concentrations of 0.09 ± 0.06 and 0.78 ± 0.57 respectively, excluding SU611, while Unit III showed densities of 1.6 ± 1.62 and 0.28 ± 0.15, respectively. Although the sediment's charcoal concentration was low, the final number of fragments obtained in some structures was statistically significant (Table 4). Preservation was poor, and numerous alteration processes were detected (Fig. 9), some of them associated with wood combustion characteristics (vitrification, radial cracks), and others with the post-depositional processes of open-air sites (rounded forms, external patina).

Taxonomic diversity was very low, and was restricted to the presence of two groups: *Pinus* and *Quercus*. In the case of *Pinus*, it was not possible to identify the species; both Aleppo pine and stone pine belong to the pinoid group in this area. The presence of plant tissue other than wood is remarkable, since several fragments of pine scales and pine nut shells were identified (Table 4). Such a low taxonomic representation is consistent with processes of anthropogenic selection, rather than charcoal produced by natural fires.

Regarding *Quercus*, the evergreen variety was identified in many cases, including species such as the kermes oak (*Q. coccifera*) or the holly oak (*Q. ilex*). When the conservation and/or size of the fragments could not be further identified at a species level, the identification remained at genus. This was also the case for specimens identified as Conifer, Angiosperm or Indeterminable.

With regard to the carpological remains, we recovered a small assemblage of charred seeds, most of which came from combustion areas (Table 5, Fig. 10). They were identified as legumes. A precise taxonomic identification was difficult because seeds do not preserve their surface features. Other charred seeds were classified as Indeterminate or Indeterminable when their state of conservation did not permit their identification. An interesting residue recovered was the remains of a fungus, probably carbonized. It corresponds to the residue of *Cenoccocum* sp., which inhabits trees and bush roots. The interpretation of this fungus is problematic, because, traditionally, its presence integrated in palaeobotanical analyses has tended to be ignored (Alonso and López 2005). It is therefore important to note its presence, because it may be related to firewood collection strategies, with the use of dead wood being a plausible hypothesis, which is consistent with the enormous contamination of wood by different fungi (Fig. 9), without ruling out that it could reflect more recent contamination.

Table 2. Results of the two Bayesian phase models for El Arenal de la Virgen site with the posterior (modelled) radiocarbon age distributions. Model 1, based on the entire radiocarbon record, has an A_{model} = 153, and Model 2, based on five radiocarbon dates, has an A_{model} = 107.1.

				Model 1			Model 2		
Phase	Sample ID	Provenance	^{14}C BP age	Modelled 95.4% range (cal a BP)		Agreement index	Modelled 95.4% range (cal a BP)		Agreement index
Phase 3	Boundary	End of Phase 3		7562	6785		7562	6779	
	Beta-473943	SU620	6560 ± 30	7560	7425	94.6	7561	7425	95.1
	Boundary	Start of Phase 3		8205	7432		8184	7430	
Phase 2	Boundary	End of Phase 2		8358	8166		8416	7780	
	Beta-493227	Level IV, top/1	7470 ± 30	8365	8220	105.7			
	Beta-493224	SU615	7480 ± 30	8381	8284	107.8			
	Beta-493226	SU604/4	7550 ± 40	8411	8340	120.8	8422	8220	106.1
	Beta-493222	SU613/2	7660 ± 30	8455	8385	122.4	8520	8385	106.8
	Beta-502077	SU612	7680 ± 30	8502	8408	118.2			
	Beta-493219	SU608/1	7700 ± 30	8525	8425	108.7			
	Beta-493223	SU623/1	7700 ± 30	8550	8450	103.2			
	Beta-243772	SU604	7750 ± 40	8574	8469	111.4			
	Beta-493225	SU613/1	7770 ± 30	8593	8491	118.1			
	Beta-493228	Level IV, top/2	7790 ± 30	8601	8536	126.5			
	Beta-473944	SU625	7850 ± 30	8625	8550	115.6			
	Beta-493221	SU613/1	7820 ± 30	8641	8559	108			
	Boundary	Start of Phase 2		8728	8561		8956	8389	
Phase 1	Boundary	End of Phase 1		9250	8707		9260	8671	
	Beta-473942	SU611	8200 ± 30	9248	9024	103.9	9249	9024	103.8
	Beta-493220	SU608/3	8220 ± 30	9286	9034	104.1	9286	9034	104.1
	Boundary	Start of Phase 1		9617	9033		9615	9032	

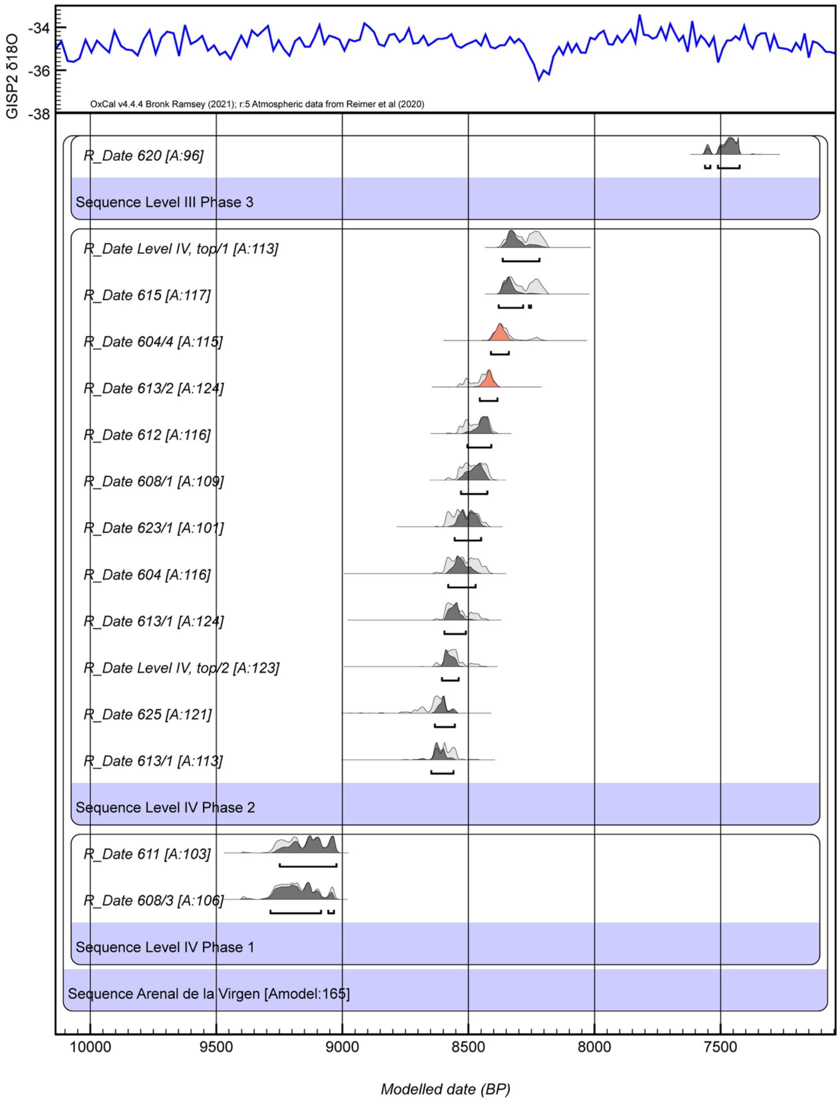

Figure 8. Multiplot of the Bayesian phase model of El Arenal de la Virgen site. The model structure is composed of three phases arranged in sequential order nested within the overall site sequence. Prior distributions (unmodelled calibrations) are shown in light colour and posterior distributions (modelled) are solid shaded areas (grey and red). The red shaded areas come from radiocarbon samples on pine cone scales. Top: GISP 2 ice core oxygen isotope ratios as a proxy of global temperatures in the northern hemisphere.

The results of the site's different phases of occupation presented some interesting differences regarding the presence of plant remains (Table 4). During *Occupation Phase 1, Early Mesolithic* (ca. 9247–9041 cal a BP), a preferential exploitation of *Quercus* wood (more than 80%) was observed. Given that the archaeobotanical results obtained were likely to be biased due to the impact of post-depositional processes, we could not rule out other possible undocumented plant resources. Nevertheless, these data showed clear trends that could be assessed based on the good availability and abundance of *Quercus* species in the environment.

During *Occupation Phase 2, Mesolithic* (ca. 8630–8292 cal a BP), conifers accounted for at least 15% of the remains. As a result, the percentage of *Quercus*, which was still dominant, fell slightly with respect to the previous phase. Similarly, the percentage of taxonomically undetermined fragments was high due to the aforementioned state of preservation (Table 4). It was interesting to note the presence of pinecone remains, especially in Phase 2. Although the absolute number of remains was not very high, it was remarkable, given the scarcity of carbonized material generally, and of pine wood in particular. Although the material was too scarce to allow any hypothesis of human management of this species, the presence of scales may be due to the fact that they were used as fuel (they are highly flammable) or for the practice of exposing the pinecones to fire to obtain pine nuts for consumption, as observed at other post-Palaeolithic sites (Badal, 1998). The presence of Fabaceae seeds has been documented for both Mesolithic phases. Although the carpological results are limited in quantitative terms, from a qualitative perspective, they provide a valuable source of information regarding gathering strategies of vegetal resources in the Mesolithic period in Iberia. The latter has been observed in the carpological record of other sites of this same chronology, such as the Santa Maira cave (Alicante, Spain) (Aura *et al.*, 2005).

Lithic assemblages: spatial distribution and morpho-technical analysis

The lithic assemblage recovered in Arenal de la Virgen over the different fieldwork seasons comprised 2106 lithic remains, scattered across the excavation area's 84 m^2. Of these, 870 were recorded in the field using the total station, whereas for the rest, 1236 spatial coordinates were randomly generated within each sub-square unit.

The spatial distribution showed an uneven scattering pattern across the excavation area (Fig. 5b). At first glance, a clear difference in the density of the remains is noticeable between the southern and the northern half of the area. The southern sector shows a denser occurrence of lithic remains whereas the northern sector displays a more disperse distribution pattern, with two minor concentrations. The first is between columns

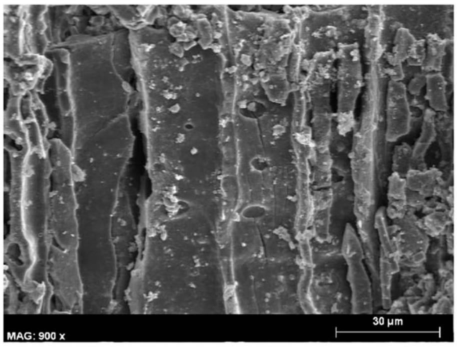

1. *Pinus* sp. Radial section x 900

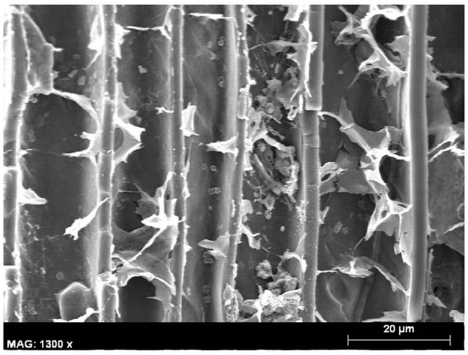

2. *Pinus* sp. Radial section x 900, altered wood

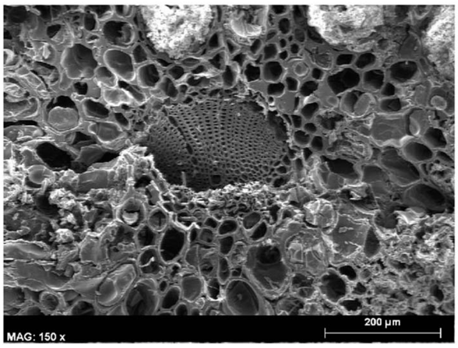

3. *Pinus* sp. scale. Cross section x 150

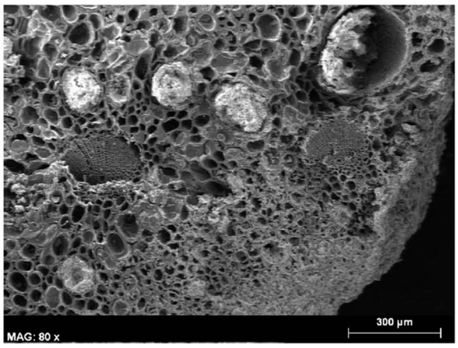

4. *Pinus* sp. scale. Cross section x 80

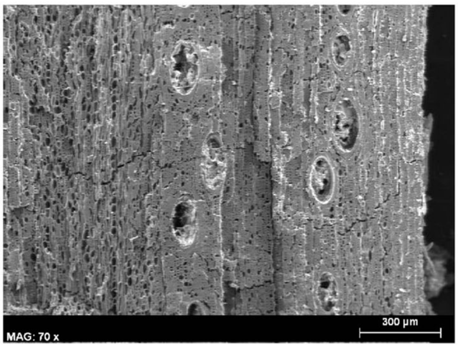

5. *Quercus* sp. evergreen. Cross section x 70

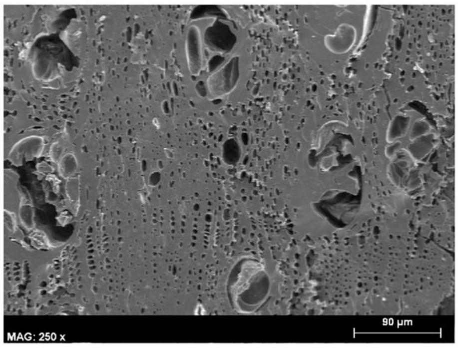

6. *Quercus* sp. evergreen. Vitrified cross section x 250

Figure 9. Scanning electron micrographs of some woody taxa identified at the Arenal de la Virgen site.

Table 3. *Span*() and *Interval*() queries for the two Bayesian phase models of El Arenal de la Virgen sequence calculated with OxCal v4.3.2 (Bronk Ramsey, 2017) (we refer the reader to the posterior probability distribution plots in Supporting materials-1, Fig. S4).

	Model 1	Model 2
Span Level IV Phase 1 (95.4% CI)	0–168	0–166
Interval Phases 1–2 (95.4% CI)	68–625	10–727
Span Level IV Phase 2 (95.4% CI)	218–397	0–180
Interval Phases 2–3 (95.4% CI)	54–872	6–882

12 and 14 and rows I and J, and the second is in excavation square I16.

To test the uneveness of the lithic assemblage's spatial distribution we performed a Clark–Evans aggregation test (Clark and Evans, 1954) based on the spatstat package (Baddeley *et al.*, 2015) in R (v.3.6.3) (R Core Team, 2020). The test yielded an aggregation index $R = 0.80048$ ($p = 0.002$), quantitatively corroborating that the lithic remains were unevenly scattered throughout the excavation area (Rabuñal, 2021).

Based on a first archaeo-stratigraphic approach, to avoid precluding the stratigraphic attribution of the lithic assemblages to each phase, all the lithic remains recovered in Units III and IV were associated with a single archaeological horizon. This horizon is of variable thickness, ranging from just 1 cm in the north sector to a maximum of 40 cm in the southern area, with a mean of 12 cm, and a gentle southeast dip. Within the archaeological horizon, it was not possible to identify archaeo-stratigraphic sub-horizons delimited by sterile layers. This trend is illustrated in Fig. 5b by four, 0.5-m-wide vertical projections in rows E, G and K as well as in column 7. This broad vertical distribution pattern can be explained by different processes, including post-depositional disturbance (trampling), erosion (deflation and colluvial activity) and pedogenesis (bioturbation) in aeolian–sandy sedimentary contexts (Butzer, 1982; Schiffer, 1987; Rolfsen, 1980; Villa and Courtin, 1983; Wood and Johnson, 1978). Particularly in the southeastern area, the co-occurrence of deflation and subsequent colluvial deposition could explain the presence of typologically related Early Mesolithic assemblages at the interface with Unit III.

Table 4. Frequencies of the woody taxa identified at El Arenal de la Virgen site.

	Early Holocene													Middle Holocene				
Phase	Phase 1 Mesolithic						Phase 2 Mesolithic							Phase 3 Neolithic				
Stratigraphic Unit	608		611		Total		604		613		615	Total		620		627	Total	
Taxa	*n*	%	*n*	%	*n*	%	*n*	%	*n*	%	*n*	*n*	%	*n*	%	*n*	*n*	%
Pinus sp.									6	10.91	1	7	5.15			2	2	3.45
Pinus (scale)							3	4.76	6	10.91	3	12	8.82					
Pinus (nutshell)	1	1.39			1	0.2												
Conifer							1	1.59	1	1.82		2	1.47			1	1	1.72
Quercus sp. evergreen	11	15.28	195	50	206	44.6	12	19.05	7	12.73		19	13.97	21	43.8	2	23	39.66
Quercus sp.	34	47.22	143	36.67	177	38.3	27	42.86	19	34.55	10	56	41.18	19	39.6	2	21	36.21
Angiosperm	12	16.67	32	8.21	44	9.5	10	15.87	6	10.91	2	18	13.24	4	8.3		4	6.90
Indeterminable	14	19.44	20	5.13	34	7.4	10	15.87	10	18.18	2	22	16.18	4	8.3	3	7	12.07
Total	72	100	390	100	462	100	63	100	55	100	18	136	100	48	100	10	58	100

Table 5. Macrobotanical remains identified in the Mesolithic phases of El Arenal de la Virgen

Taxon	Phase 1: Mesolithic SU608	Phase 2: Mesolithic				Total
		SU604	SU613	SU612	Level IV	
Fabaceae	1	1	2			4
Indeterminate		1		1		2
Indeterminable					1	1
Cenoccocum					1	1
Total	1	2	2	1		10

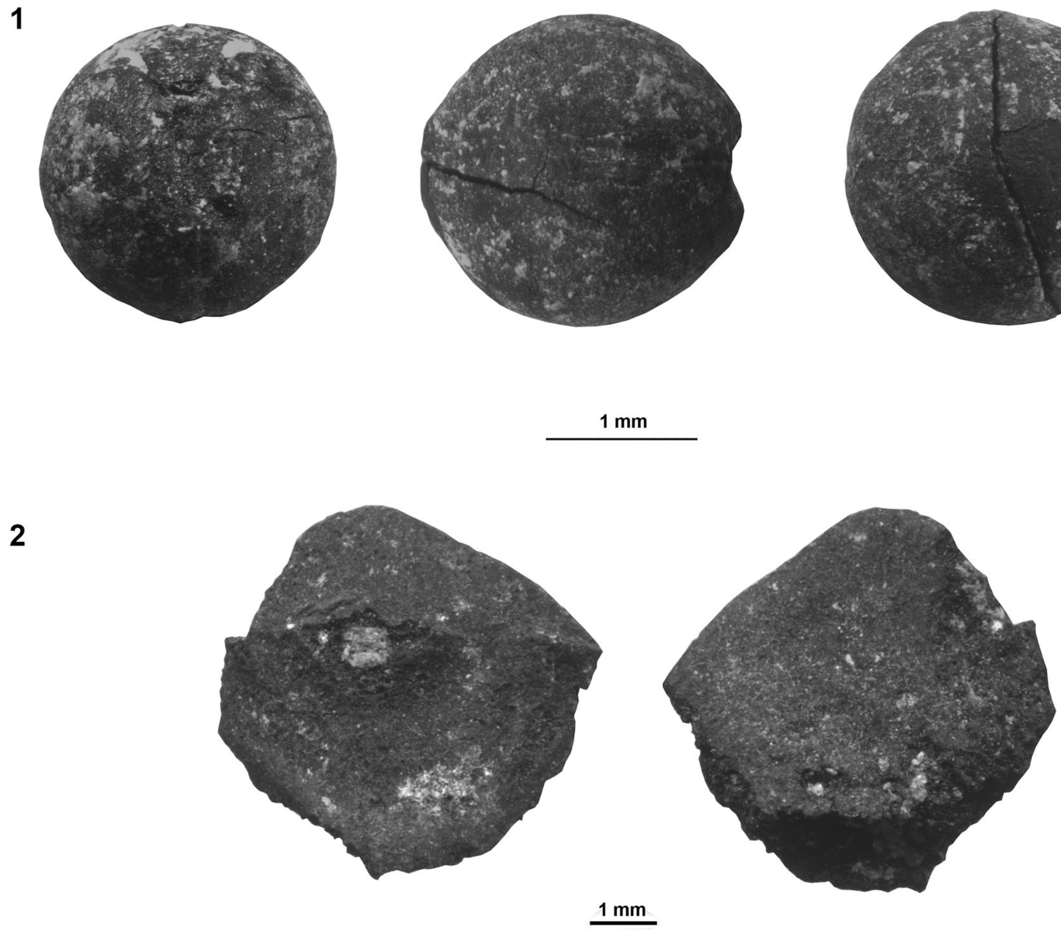

Figure 10. Charred seed of Fabaceae from SAU613; 2. *Pinus* sp. scale from SU604.

Works on lithic refitting (Rabuñal, 2021) allow the exclusion of long-distance movements of lithic materials indicative of secondary deposition processes. To date, 38 sets of connections have been identified, consisting of 15 refits, 13 conjoins and 10 thermal conjoins. These connections involve a total of 86 artefacts, representing 8.35% of the over-10-mm material. Mean distances for these connections are 0.94 m for the refits, 1.45 m for the conjoins and 0.84 m for the thermal conjoins. The spatial distribution of these connections (Fig. 5c) is consistent with that outlined in the distribution of the lithic assemblage and reinforces the association of the lithic remains with the archaeological structures of the two Mesolithic phases. In particular, during Phase 1, two short-distance connections were recorded in SU611, whereas in Phase 2, short-distance connections were also recorded in SSUU613, 615 and 604.

The lithic assemblage was mainly composed of chert (>99%), associated with different reduction and configuration strategies. A very marginal presence of other lithic raw materials, such as limestone, quartzite and sandstone was also documented, in the form of hammers or hammer fragments and small debris.

Morpho-technical analysis of the lithic assemblage (Rabuñal, 2021) showed a predominance of micro-debris (<10 mm; 49.62%). Overall, lithic reduction was overwhelmingly dominated by flake production strategies: unifacial (unipolar and bipolar opposed), bifacial (orthogonal and multipolar centripetal), multifacial (orthogonal and multipolar) and bipolar on anvil. In contrast, evidence of blade/bladelet debitage – whether cores, blanks or preparation products – was extremely scarce (<1%) in the lithic assemblage.

Among the knapping products, complete flakes were the most abundant (21.46 %), whilst flake fragments represented 16.38 %. A total of 84 retouched artefacts – mainly configured on flake blanks – were identified in the lithic assemblage. They corresponded to a reduced set of typological groups, clearly dominated by notches and denticulates, endscrapers and non-geometric microliths. Overall, the technical and typological characteristics of the lithic assemblage fit with those of the Mesolithic of Notched and Denticulated tradition (Alday, 2006), confirming the previous chrono-cultural attribution (Fernández-López de Pablo *et al.*, 2011). However, detailed techno-typological analysis of the lithic assemblage revealed some differences between Phase 1 and Phase 2 (Rabuñal 2021, Rabuñal and Fernández-López de Pablo, 2022). For Phase 1, we find a reduced set of retouched artefacts configured on large and thick (>8 mm) blanks (Fig. 11). In contrast, for Phase 2, the typometry of the configured tools shows a much higher variability, from large denticulates on thick flakes to non-geometric microlithic armatures configured on micro-flakes (Fig. 12). It should be stressed that the modelled radiocarbon chronology for Phase 2 (8630–8292 cal a BP) overlapped with the first Late Mesolithic industries in the Tardenoisian tradition in the Iberian Mediterranean region, characterized by bladelet debitage systems, the microburin technique and the dominance of trapezoid microliths (Martí *et al.*, 2009; García-Puchol *et al.*, 2018). In the Arenal de la Virgen lithic assemblage, such techno-typological traits are completely absent.

Palaeoecology

The vegetation dynamics substantiated by the new Bacon depth model is summarized in Fig. 13. For the Early Holocene section (from 9.1 to 8.3k cal a BP), prior to the 8.2k cal a BP climatic event, the Villena palaeolake was surrounded by

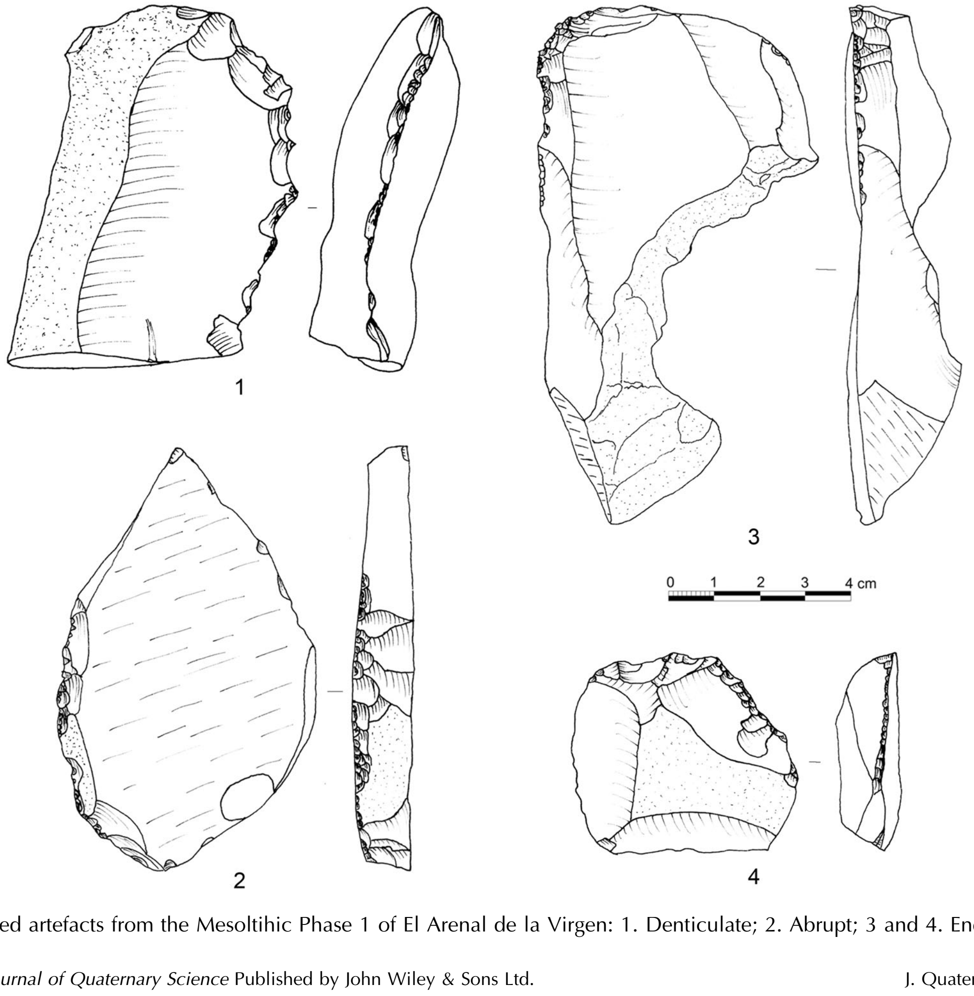

Figure 11. Retouched artefacts from the Mesoltihic Phase 1 of El Arenal de la Virgen: 1. Denticulate; 2. Abrupt; 3 and 4. Endscrapers.

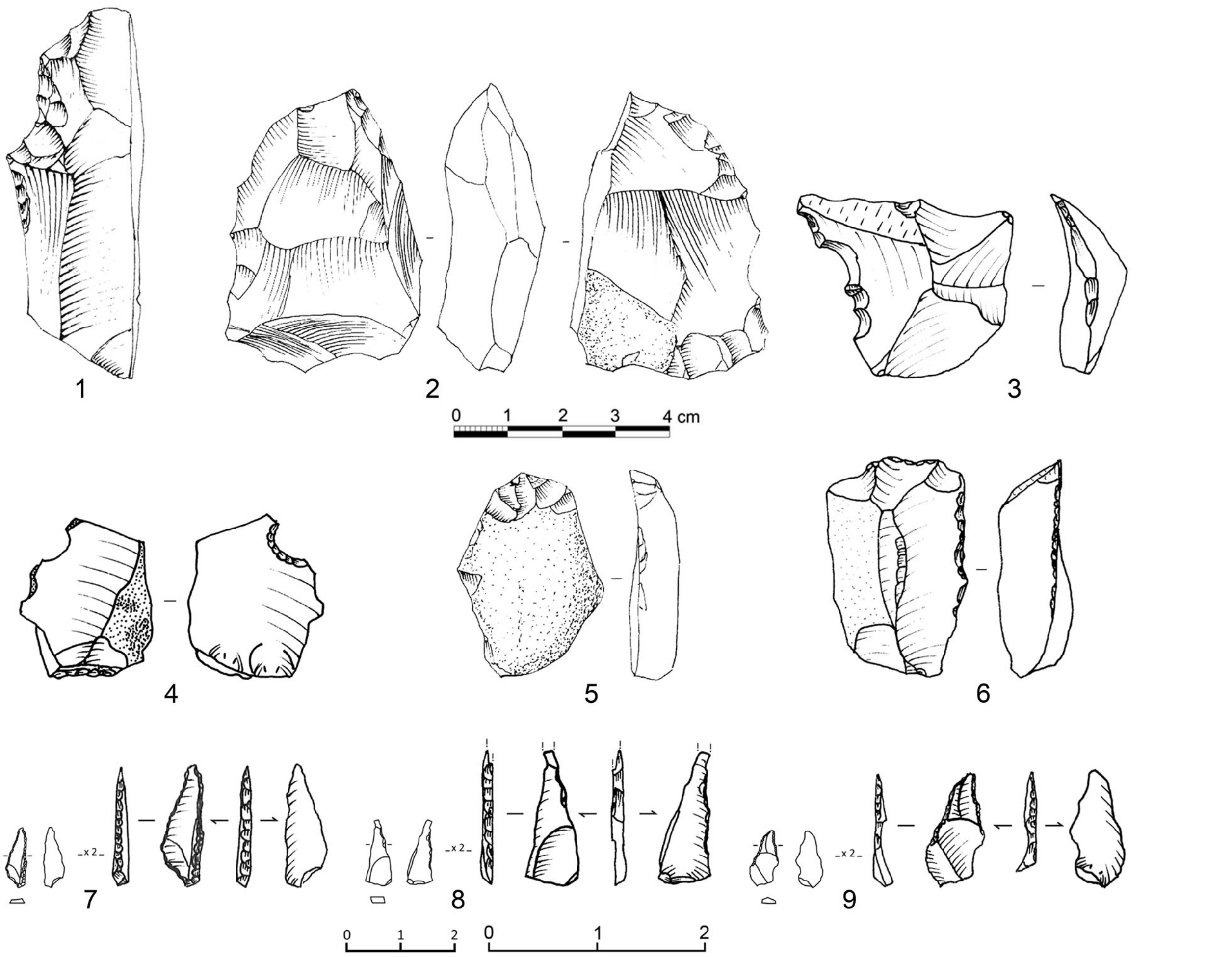

Figure 12. Retouched artefacts from the Mesolithic Phase 2 of El Arenal de la Virgen: 1, 2 and 3. Denticulates; 4. Notch; 5 and 6. Endscrapers; 7, 8 and 9: non-geometric microliths.

mixed Mediterranean forests of oaks (deciduous and evergreen *Quercus*) with thermal taxa, such as the wild-olive (*Olea*) and green olive trees (*Phillyrea*) (Fig. 13, top). The lake shore was colonized by hazel (*Corylus*), willows (*Salix*), ash trees (*Fraxinus*), alder (*Alnus*) and elms (*Ulmus*).

In contrast, during the formation of Unit III, which overlaps the chronological span of the 8.2k cal a BP cold climatic event, the pollen records of the Villena palaeolake show evidence of increasing aridity. During this episode, we find a decline in oaks and the pollen taxa of open forests such as pines (also identified above in the archaeobotanical record) and an increase in xerophilous scrub taxa (e.g. *Erica*). This change seems to be clearly associated with a general decrease in precipitation, which, in turn, is additionally supported by the reduction of lake shore trees (*Corylus*, *Salix*, *Ulmus*, *Alnus*), sedges (hygrophytes Cyperaceae) and ferns (monolete and trilete spores) in the diagram. Finally, we found a decrease in grass taxa such as Poaceae, Cerealia-type and *Lygeum*, and an increase in the herbaceous taxa Amaranthaceae. In this context, it is of note that the appearance of brackish taxa (*Ruppia*) immediately before the 8.2k cal a BP event supports a significant increase in salinity over that period.

The Salines playa-lake, just 10 km south of the Arenal site, shows a very similar vegetation dynamic (Fig. 13, bottom). During the Mesolithic occupation phase, the surrounding forests of Salines were also dominated by mixed oaks and pines, but with a higher relative abundance of oaks than in Villena. In Salines, the lake-shores were colonized by hazel (*Corylus*), ash trees (*Fraxinus*), alder (*Alnus*) and elms (*Ulmus*). We observed an increase in Mediterranean taxa, particularly the wild olive (*Olea*) and species of green olive trees (*Phillyrea*) from 8.8k cal a BP onwards in both records. This signifies a gradual increase in aridity, which culminated during the 8.2k cal a BP climatic event. Such a rise in aridity is also corroborated by the appearance of brackish *Ruppia*, an increase of Amaranthaceae, and a decrease of other taxa such as Poaceae, *Typha-Sparganium*, ferns and Cyperaceae. These results are additionally supported by the aridity quotients of Salines and Villena published in Burjachs *et al.* (2016) (Fig. 14). Overall, cessation of Mesolithic occupation at the site correlates well with the 8.2k cal a BP event, which, at a local scale, is manifested by a dominance of open pine forests, a decrease of oaks and lake shore trees, and an increase of brackish *Ruppia*.

Palaeohydrology

The local-scale palaeoenvironmental evolution (Fig. 14) drawn from the Early Holocene sections of the Villena and Salines playa-lake records (Jones *et al.*, 2018; Burjachs *et al.*, 2016) was compared with the global $\delta^{18}O$ GISP2 curve (Stuiver et al.,, 1995; Grootes and Stuiver, 1997; Rasmussen *et al.*, 2014) and the pollen-inferred regional pluviometric index (Ip) for the Alborán Sea (Fletcher *et al.*, 2010). The Salines aridity quotient curve was plotted according to the raw data, without any smoothing or rolled mean, as previously published by Burjachs *et al.* (2016).

X-ray diffraction results showed a growing aridity trend as of ca.9.1k cal a BP, denoted by the drop in magnesian calcite, a proxy for water stability in the lake system. Such a decrease was concomitant with increasing aragonite values (Julià *et al.*, 1998) and quartz (Clark *et al.*, 2002), signifying lower lake levels. The

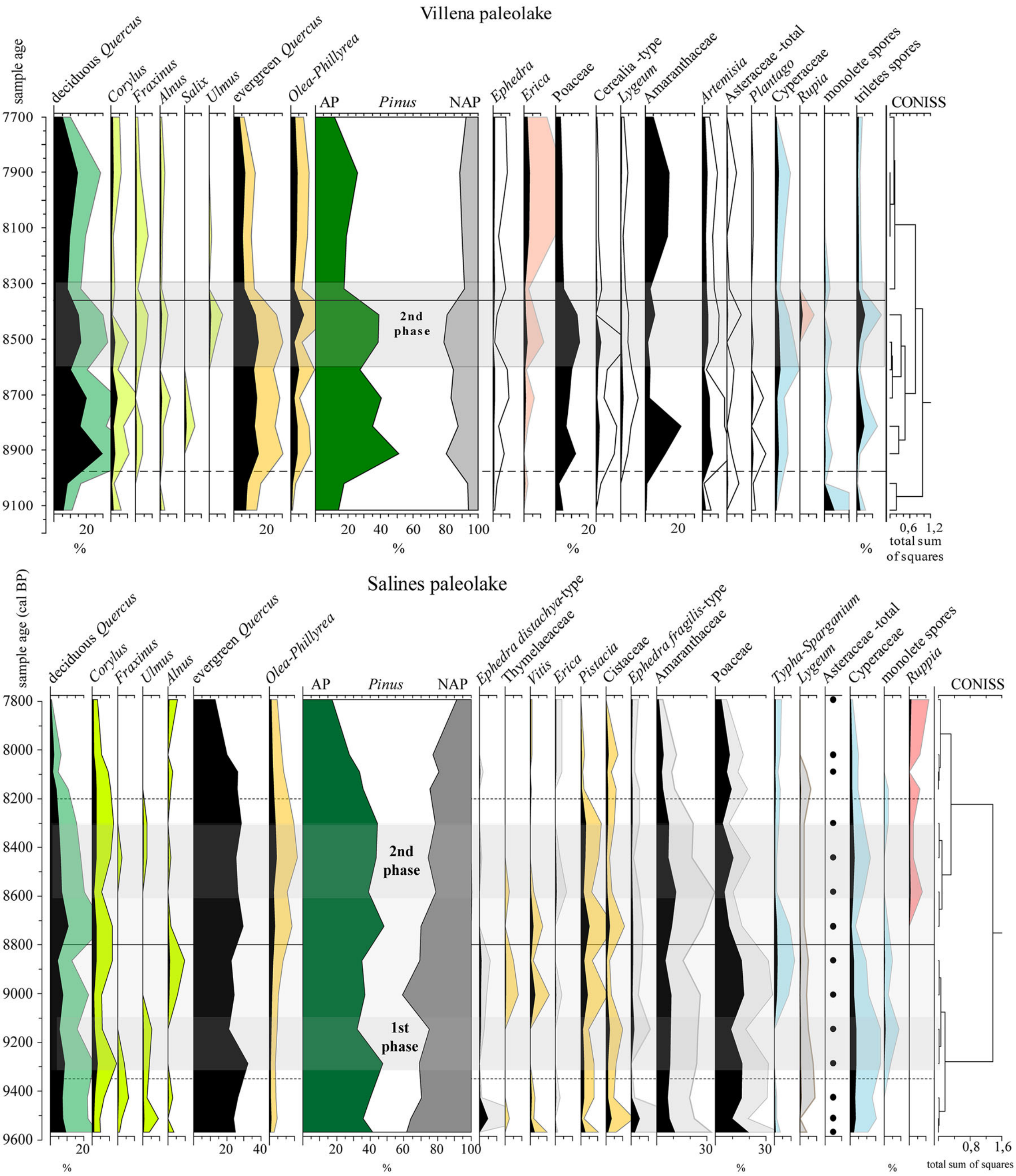

Figure 13. Pollen diagram of the Villena palaeolake (top) and Salines (bottom) based on selected taxa chronologically constrained to the Arenal de la Virgen chronology. The dots mark rates <1%. The colour plots correspond to an exaggeration of the real values (black). Horizontal shaded areas represent the radiocarbon-modelled Mesolithic occupation phases of El Arenal de la Virgen.

maximum peaks in aragonite and quartz were dated to ca. 8.6 k cal a BP, in agreement with the drop in precipitation observed in the Salinas playa-lake and the Alborán deep-sea core, based on pollen indexes (Ip). In addition, the highest calcium dolomite values were observed at ca. 8.3k cal a BP, when magnesian calcite reached its lowest values.

In summary, a period of environmental stability could be found between ca. 9.4 and 8.2k cal a BP, coinciding with the maximum ^{18}O isotope values in the Greenland GISP-2 record. Such stability was locally manifested in the aridity quotients of Salines, the Salines precipitation index and the Villena palaeolake's X-ray data. This was despite a long-term trend of growing aridity with several aridity peaks starting at ca. 8.6k cal a BP, and culminating with the 8.2k cal a BP event. Such a trend is consistent with the precipitation index (Ip) observed at a regional scale in the Alborán deep-sea record. The end of the Mesolithic occupation at the Arenal de la Virgen site fits well with the onset of the 8.2k cal a BP event according to the Greenland records (8300+10/−40 a b2k) (Rasmussen *et al.*, 2014), when the Salines record shows a significant increase in the aridity quotient and the Villena palaeolake presents a peak in calcium dolomite.

Discussion

Archaeological sequence and occupational evidence

The new excavations at Arenal de la Virgen have considerably increased the body of occupation features, lithic and palaeobotanical assemblages documented in previous works

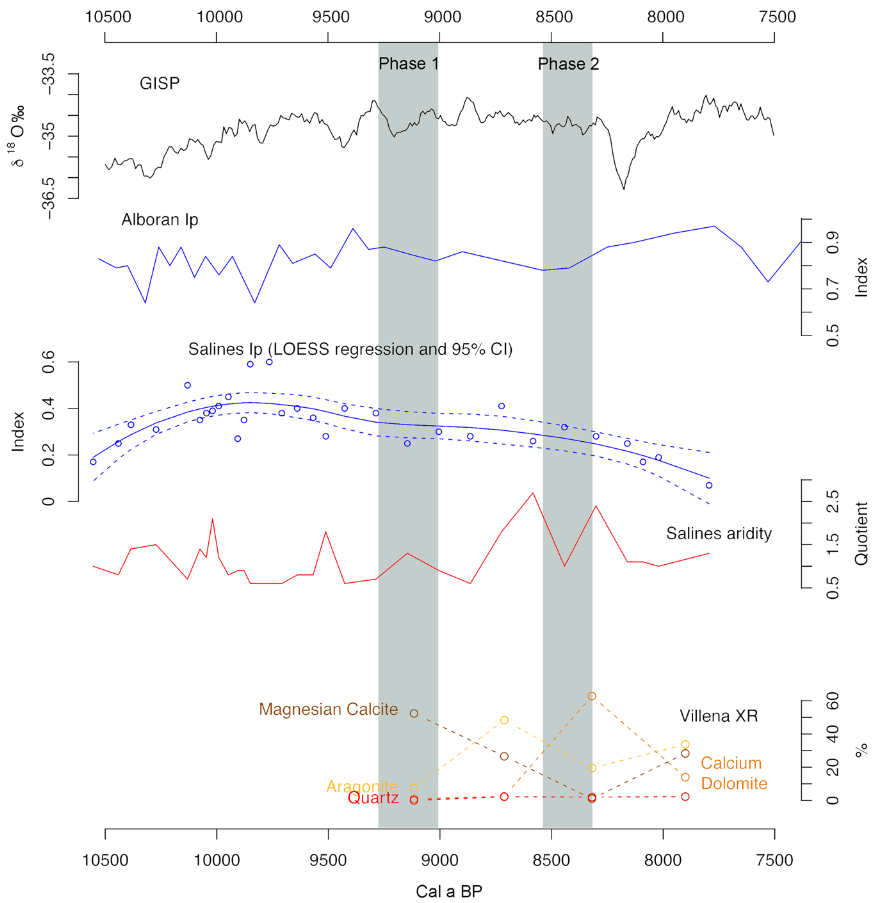

Figure 14. Multi-proxy palaeohydrological reconstructions in the Upper Vinalopó Valley compared with the two Mesolithic occupation phases of El Arenal de la Virgen. Two local aridity events (10.3 and 9.4k cal a BP) before the Mesolithic occupations of Arenal de la Virgen site. The 10.28–10.4k cal a BP event *sensu lato* (Bond *et al.*, 1997; Cacho *et al.*, 2001; Combourieu-Nebout *et al.*, 2009; Zielhofer *et al.*, 2017) is manifested by an increase in the aridity quotient of Salines (adapted from Burjachs *et al.*, 2016) and a decrease in the pluviometric index (Ip) of Alborán (adapted from Fletcher *et al.*, 2010); the aridity quotient, however, is most pronounced at 8.6k and at 8.2k cal a BP. This 8.2k cal a BP aridity peak is globally correlated with a decrease in temperature in the GISP2 $\delta^{18}O$ isotopic record (Stuiver, 1995; Grootes and Stuiver, 1997) and, more locally, by a pronounced increase in calcium dolomite at 8.3k cal a BP in the X-ray diffraction results (XR) (adapted from Jones *et al.*, 2018). Multiproxy data is available at the Zenodo repository of this article.

(Fernández-López de Pablo *et al.*, 2011a). Both the sedimentary characterization of the stratigraphic sequence and the application of a new programme of ^{14}C AMS dates allowed us to distinguish two Mesolithic occupation phases within Unit IV, whose lithic assemblages correspond to the Notched and Denticulated Mesolithic. For the first occupation phase (9242–9041 cal a BP), the information derived from archaeological features seemed to be restricted to the northern area, consisting of two hearthpits. One of them was interpreted as a possible dumping feature based on the high density of charcoal remains. In contrast, the second phase (8630–8292 cal a BP) was widely documented over most of the excavation area, with at least three combustion features, a pit and a possible altered dwelling with a posthole containing a 40 -cm-long limestone block. As briefly discussed earlier, the interpretation of SU604 as a pit-dwelling requires caution because this feature does not represent a primary depositional context. Rather, the presence of combustion residues such as thermo-altered limestone clasts, vegetal charcoals as well as thermo-altered lithic artefacts, ochre and monospecific accumulations of the edible land snail *Sphincterochila candidissima* (Fernández-López de Pablo *et al.*, 2011b) indicates a complex formation process. The most parsimonious explanation is the interaction of occupational residues, produced during recurrent use of this space, with soil formation processes. The chronological association between SU604 and the posthole with the limestone wedge, over timescales of just a few generations, is supported by the occupation span of the second phase (0–158 years at a 95.4% CI) inferred from our second Bayesian chronological model, built on radiocarbon determinations from pinecone scales. According to this, the posthole might be interpreted as a vertical feature, giving structure to a space of domestic activities used along successive occupation episodes that resulted in a palimpsest. In sum, the occupational evidence for Phase 2 allows for a first appreciation of the site structure as a part of a campsite. This campsite would have comprised a sheltered (presumably domestic) area and an adjacent activity area with different combustion features, and other latent combustion features suggested by the spatial distribution of the burnt lithic remains (Rabuñal, 2021). The taxonomic composition of charcoal assemblages recovered in the combustion and habitational features of Phase 2 shows a clear dominance of *Quercus* and the probable selection of pine scales as fuel. This, in addition to the presence of Fabaceae seeds, qualitatively supports the presence of activity areas associated with the combustion features.

Information about the seasonal patterns of occupation is still very limited, given the null preservation of faunal remains and the paucity of fruit seeds. In a previous study, we suggested a spring and/or autumn occupation season according to the ethology of *S. candidissima* land snails (Fernández-López de Pablo *et al.*, 2011). This remains to be confirmed by ongoing sequential intra-shell isotopic $\delta^{18}O$

analyses (Yanes and Fernández-López de Pablo, 2017). More detailed intra-site studies focused on detailed geoarchaeological analyses of features (Polo-Díaz *et al.*, 2022), and the spatial distribution of lithic assemblages (Rabuñal *et al.*, 2022) will be published elsewhere, providing additional evidence of site formation processes, site structure and behavioural patterns.

A detailed comparative study of our excavation results with other Iberian and European open-air Mesolithic sites is beyond the scope of the present article. Nevertheless, it is worth briefly mentioning here its significance considering the level of information currently available for the Notched and Denticulate Mesolithic in the Iberian Mediterranean region. In this area, the number of open-air sites with published habitation features, spatial distribution of archaeological materials and palaeobotanical evidence is restricted to Font del Ros (Martínez-Moreno and Mora, 2011), Sota Palou (C.R.E.P.S., 1985) and Parque Darwin (Escobar, 2010).

In the Font del Ros site, Unit SG has provided lithic assemblages, 10 combustion structures and two pits, defining two main activity areas over an excavation surface of 1200 m^2 dated to ca. 10200–9700 cal a BP based on AMS ^{14}C dates on *Corylus avellana* shells (Martínez-Moreno and Mora, 2011; Roda Gilabert *et al.*, 2016). The spatial distribution of lithic artefacts, combustion features, ground stone tools and hazelnuts indicates a residential camp function, with spatially differentiated domestic activity areas. For Sota Palou, the occupational evidence is more limited, even though it has been reported in detail (CREPS, 1985; Carbonell and Mora, 1985). An occupation floor, 15 cm deep on average, was excavated at Level 10 over 40 m^2. The documented body of archaeological features encompasses two combustion features, forming shallow pits with rubified sediment and charcoals, a sitting cobble, and two post bases. The presence of a latent dwelling that extends outside the excavation area was hypothesized, based on abrupt changes in the density of archaeological materials and the spatial distribution of posts (Carbonell and Mora, 1985). However, the radiocarbon resolution from Level 10, with two conventional ^{14}C dates of charcoal aggregates with wide standard errors – 8540 ± 180 and 9060 ± 360 BP – does not allow us to evaluate such a hypothesis. As in Font del Ros, archaeological assemblages document the presence of carbonized remains of hazelnuts and groundstones.

Finally, regarding Parque Darwin, the available information comes from two studies on the lithic and palaeobotanical assemblages (Escobar, 2010; Berihuete *et al.*, 2017), with very preliminary descriptions about occupation features, the spatial distribution and the radiocarbon record. According to the site planimetry, which covers an excavation surface of ~70 m^2, a total of 21 archaeological features were identified as combustion structures, postholes and a 'possible dwelling' (Escobar, 2010). At least 14 of these archaeological features correspond to combustion features providing charcoal assemblages (Berihuete *et al.*, 2017). The AMS radiocarbon chronology from archaeological features 8 and 11 yielded statistically significant different ages, 8920 ± 40 BP (10 200–9910 cal a BP) and 8470 ± 70 BP (9550–9400 cal a BP). Such chronological differences are indicative of a palimpsest, whose formation time and internal phasing remain to be determined. This synthetic review shows that palimpsests spanning few centuries are common in other open-air sites of the Iberian Peninsula, and underlines the need to develop new radiocarbon dates and bayesian chronological models to determine the internal phasing and establish their chronological boundaries.

Correlation between the occupational sequence and local-scale paleoenvironmental dynamics

The stratigraphic sequence of El Arenal de la Virgen shows a sedimentary succession of alternating phases formed under arid and relatively wetter conditions, which could be correlated with environmental dynamics observed both at local and regional scales. The sedimentary context of the Mesolithic occupations was formed by sands, but with evidence of pedogenesis, signifying more stable and humid conditions, as locally recorded by the Villena and Salines palaeoecological sequences (Burjachs *et al.*, 2016; Jones *et al.*, 2018). The Bayesian radiocarbon model of the Arenal sequence reveals two different Mesolithic occupation phases within Unit IV, both with lithic assemblages taxonomically attributed to the Notched and Denticulated Mesolithic. The two occupation phases were separated by a chronological hiatus of about 700 calendar years, reflecting sedimentary discontinuities of colluvial origin, according to the micro-stratigraphic evidence (Supporting Information, Fig. S2).

Cessation of the Mesolithic occupation at the Arenal site is clearly associated with the beginning of Unit III deposition. The contact between Units IV and III is of major relevance in this study. It manifested as an abrupt shift from soil formation processes to the accretion of aeolian sands. This change reflects the onset of a new arid phase, chrono-stratigraphically correlated with the 8.2k cal a BP event, reflected at a local scale in the Salines and Villena pollen and sedimentary records. The latter shows an expansion of conifers, halophytes (e.g. Amaranthaceae), and brackish (e.g. *Ruppia*) and xerophilous taxa (e.g. *Ephedra*, *Erica*), all of which are indicators of increasing aridity, added to the aridity quotients published in Burjachs *et al.* (2016).

Independent chronological models derived from the stratigraphic sequence of Arenal and the revised section of the Villena palaeolake show that the beginning of the deposition of Unit III was associated with an abrupt increase in the lake's hypersaline conditions, during the accepted chronology of the 8.2k cal a BP event. As reported before, this change in hydrology is also manifested in the Salines record, 11 km from the Arenal site, and identified in vegetation patterns. A notable discussion point regarding the evaluation of the impact of aridity in Mesolithic communities is to determine whether the local signal associated with the 8.2k cal a BP differs from ongoing, millennial-scale, climatic trends. Here, we must take into consideration the sampling resolution of the local environmental proxies for the period 9.2–7.8k cal a BP. With four data points, the resolution of the X-ray data of the Villena palaeolake does not allow to precisely estimate the exact duration of aridity pulses. However, it must be noted that the age of the calcium dolomite peak (8.3k cal a BP) is coeval with a peak in the aridity quotient in the better-sampled (with 10 data points) record of Salines. According to this evidence, the Villena and Salines lake systems did not recover to 8.2k pre-event conditions but aridity persisted in the Upper Vinalopó during the mid-Holocene ca. 7000 cal a BP (Jones *et al.*, 2018). This is consistent with recent precipitation reconstructions for SE Iberia based on speleothem records (Budsky *et al.*, 2019) suggesting enhanced dry spring/summer conditions spanning 9.7–7.8k cal a BP.

The formation of Unit III, whose deposition began during the 8.2k cal a BP climatic event according to the results of the Bayesian chronological model, implied a mixed and very probably alternating dynamics of aeolian accretion and run off linked to lake level oscillations of the nearby Villena palaeolake (Jones *et al.*, 2018). Subsequent Neolithic occupations were recorded within Unit III, even though the

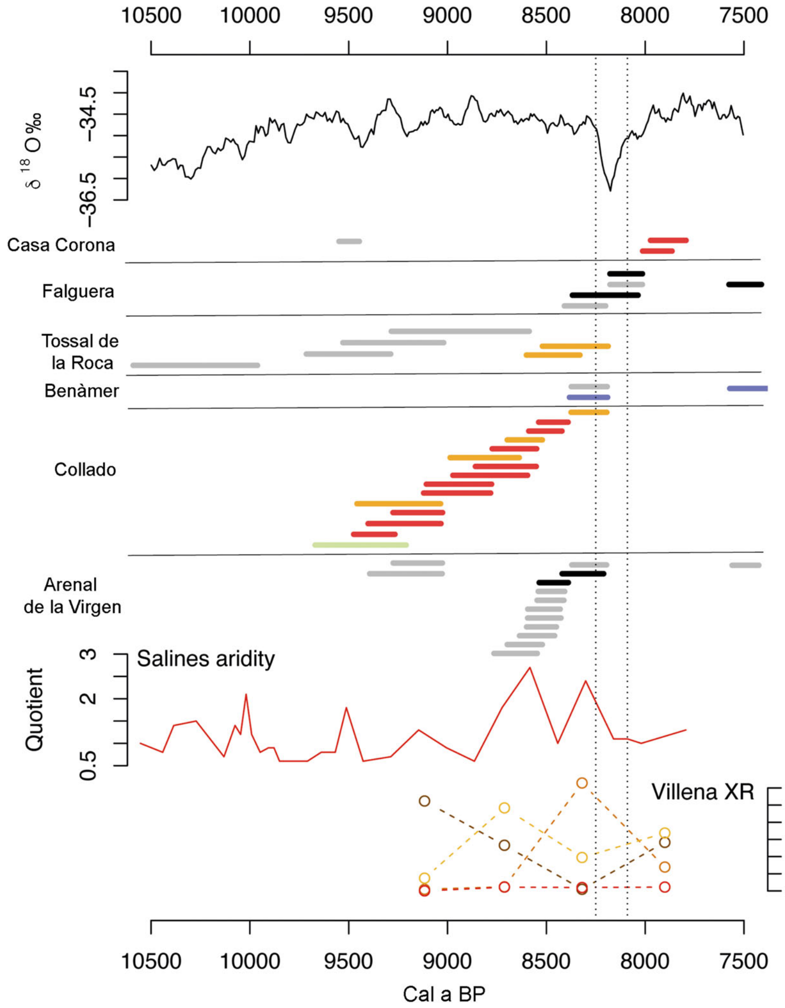

Figure 15. Multi-plot with the radiocarbon evidence of the discussed sites from the central Mediterranean region of Iberia plotted against the GISP2 δ^{18}O isotopic record (Stuiver, 1995; Grootes and Stuiver, 1997), Salines aridity quotient and the Villena palaeolake X-ray diffraction (XR) data. Horizontal bars depict the 95.4% CI calibrated chronological ranges according to different radiocarbon samples (red: human remains; orange: faunal remains; black: seeds or pine cone scales; grey: charcoal; blue: pollen concentration; light green: *Cerastoderma glaucum* shell). Arenal de la Virgen, Falguera and Benàmer show Early Neolithic reoccupations dated to ca. 7500 cal a BP. Readers are referred to the Supporting Information (Table S3) for the radiocarbon list.

archaeological evidence in the excavated area is very limited, without diagnostic potsherds or lithic artefacts. Even though the date of SU620 is based on a single charcoal sample (and therefore subject to a certain degree of chronological uncertainty), both the radiocarbon age of the features associated with Unit III and especially the typology of feature 627 agree with an Early Neolithic (*senso latu*) chronological attribution. This, in turn, is consistent with the relative chronology provided by surface findings of Cardial pottery in the crop fields adjacent to the exaction area (Soler, 1965; Fernández-López de Pablo *et al.*, 2008).

In the broader context of the central Mediterranean region of Iberia (Fig. 1), the end of the Mesolithic occupation at Arenal de la Virgen coincides with the cessation of radiocarbon-dated activity in other Postglacial sites such the Tossal de la Roca rockshelter (Cacho *et al.*, 1995; Cacho and Jordà-Pardo 2009) and, especially, the open-air sites of El Collado and Benàmer (Fig. 15, and Supporting Information 6). The most relevant example is the El Collado site, located in the southern sector of the Valencian gulf, 80 km from El Arenal de la Virgen. This site has a rich archaeological deposit with lithic, faunal and mollusc assemblages (Aparicio 2008; Fernández-López de Pablo and Gabriel 2016; Fernández-López de Pablo *et al.*, 2015) and 14 Mesolithic burials. Its stratigraphic sequence, recently revised through an extensive radiocarbon dating programme on human and faunal remains from all the stratigraphic layers (Fernández-López de Pablo 2016; Gibaja *et al.*, 2015), spans ca. 9400–8200 cal a BP.

Benàmer is located ca. 50 km from El Arenal de la Virgen, in which rescue excavations uncovered Late Mesolithic deposits (about 0.5 m thick) over an area of 200 m^2 (Torregrosa *et al.*, 2011). Two radiocarbon determinations (Supporting Information, Table S3) made on charcoal and pollen show statistically identical radiocarbon ages for the Late Mesolithic phase (ca. 8374–8192 and 8383–8190 cal a BP), in agreement with the lithic typology characterized by the dominance of trapezes with abrupt retouch. The site lacks evidence of subsequent Final Mesolithic occupations, suggesting the end of the Mesolithic presence along the chronological span of the 8.2k cal a BP event. This interruption of the Mesolithic occupation at Benàmer was concomitant with the deposition of aeolian sands, signifying an increase of aridity (Ferrer, 2011). An Early Neolithic phase has been dated to 6575 ± 50 BP (7572–7367 cal a BP) on a pollen concentration sample, which is consistent with the Cardial ceramic component of the site, showing a reoccupation by early farmer communities. In the Falguera rockshelter, two Late Mesolithic layers Xa and VIIIa are separated by an occupation hiatus of 20–25 cm depth, during the formation of Layer X (García-Puchol and Aura, 2006) and Layer IX that correspond to a 5-cm-thick layer of fluvial gravels. In a previous work we discussed the potential relationship between this occupational hiatus with the 8.2k cal a BP event (Fernández-López de Pablo and Jochim 2010). In sum, the radiocarbon evidence from open-air sites located in this regional unit suggests a wider regional impact of aridity on Mesolithic settlement systems during the onset of the 8.2k cal a BP event. Note that this interruption pattern in the occupational sequences is documented in open-air sites in different geomorphological settings and sedimentary regimes as well as in a rockshelter. It is interesting to note that the archaeological sites of Benàmer, Falguera and Arenal de la Virgen show Early Neolithic cultural layers after an occupational hiatus spanning the 8.2k cal a BP climatic event and the Final Mesolithic. In the case of the Serpis River Valley, where Benàmer, Falguera and El Collado are located, different studies have suggested that this decline on the terminal Mesolithic settlement was forced by the effects of the 8.2-ka event as well as the decrease in environmental carrying capacity in coastal areas due to postglacial flooding of coastal plains and the significant decrease of coastal lagoon biotopes (Fernández-López de Pablo 2016; Brisset *et al.*, 2018; Brisset and Fernández-López de Pablo 2022). The archaeological evidence supports that the subsequent Neolithic transition in this area involved the rapid spread of farming communities ca. 7.6–7.5k cal a BP in river valleys that were unoccupied, or very marginally occupied, by Mesolithic populations.

At the local scale of the Upper Vinalopó Valley, the interruption of the Mesolithic occupations at Arenal de la Virgen does not seem to imply the abandonment of this area, but rather a decrease in occupational intensity, coinciding with maximum peaks in aridity in the Villena palaeolake. Furthermore, the open-air site of Casa Corona, located 6 km to the north of Arenal de la Virgen, has provided two Late Mesolithic burials directly dated to 8.0–7.8 ka (Fernández-López de Pablo *et al.*, 2013). However, recent extensive fieldwork undertaken in 2014 and 2017 at this site, covering a 500-m^2 excavation surface adjacent to the Late Mesolithic burials, has confirmed the lack of new funerary evidence. This, in turn, is consistent with the study of lithic assemblages (Rabuñal, 2021) reporting the presence of trapezes but the lack of final Mesolithic assemblages with 'Cocina-type' triangles.

Conclusion

This work shows the potential of integrated archaeological and palaeoecological research targeting Early Holocene open-air sites in aeolian sandy sedimentary contexts in Mediterranean biomes. At Arenal de la Virgen, the interaction between different sedimentary processes (colluvial and aeolian sedimentation, cultural deposition and disturbance, run off and aeolian deflation) with pedogenic processes have led to the formation of a palimpsest, and prevented good preservation of organic remains. However, the application of previously defined fieldwork and post-excavation analytical protocols has allowed us to disentangle its occupation sequence, identifying cultural and natural site formation processes, extracting palaeoethnographic information within each occupation phase, and correlating its occupation history with palaeoenvironmental dynamics inferred from local palaeoecological records.

Using open-air archaeological data at local and regional scales, our work provides solid stratigraphic and chronometric evidence of the impacts of aridity on Mesolithic settlement systems during the 8.2k cal a BP climatic event in the Iberian Mediterranean region. This is especially relevant given that in this area of the Western Mediterranean, as in other regions of Southern Europe, the archaeological record has been traditionally biased in favour of rockshelter-oriented research, very often affected by sedimentary gaps (Berger and Guilaine 2009, Alday *et al.*, 2018). By expanding the focus to the open-air archaeological record, in addition to rockshelter research, we can achieve a broader and more integrated understanding of Early Holocene socio-ecological dynamics, correcting previous research biases and addressing the impacts of ACEs on patterns of human occupation.

Acknowledgements. This research is primarily part of a project that has received funding from the European Research Council (ERC) under the Horizon 2020 research and innovation programme (Grant agreement No. 683018) to JFLdP. Additional analyses on the pollen data sets have been produced in the context of the research project HAR2017-88503-P supported by the Spanish Ministry of Science and Innovation. JFLdP is additionally supported by the Plan Gen-T programme (Ref.CIDEGENT-18/040) from the Generalitat Valenciana. JRR is currently supported by a Margarita Salas fellowship (ref. MARSALAS21-22) at the University of Alicante , and AP-D is holder of a María Zambrano fellowship at the University of the Basque Country (UPV/EHU) both funded by the European Union-Next Gene and the Ministry of Universities (Government of Spain). Authors thank the constructive comments of two anonymous reviewers on previous versions of the manuscript, as well as the technical assistance of Antoni Canals, Francisco Javier García-Vadillo and Ethel Allué during the fieldwork.

Data availability statement

The data that support the findings of this study are openly available in Zenodo at https://zenodo.org, reference number https://zenodo.org/badge/DOI/10.5281/zenodo.6607582.

Author contributions—**Javier Fernández-López De Pablo**: Conceptualization; Investigation; Funding acquisition; Writing - original draft; Writing - review & editing; Project administration; Supervision; Methodology; Formal analysis; Data curation; Visualization. **Ana Polo-Díaz**: Investigation; Writing - original draft; Methodology; Formal analysis; Writing - review & editing; Data curation; Visualization. **José Ramón Rabuñal**: Investigation; Writing - original draft; Writing - review & editing; Methodology; Formal analysis; Data curation; Software; Visualization. **Magdalena Gómez Puche**: Investigation; Writing - original draft; Writing - review & editing; Methodology; Software; Formal analysis; Data curation. **Yolanda Carrión Marco**: Investigation; Methodology; Formal analysis; Writing - review & editing; Writing - original draft. **Ana Cantó**: Investigation; Writing - original draft; Methodology; Visualization; Formal analysis. **Rowan Mclaughlin**: Investigation; Visualization; Methodology; Software; Formal analysis; Writing - original draft. **Carlos Ferrer**: Investigation; Writing - review & editing. **Francesc Burjachs**: Conceptualization; Investigation; Writing - original draft; Writing - review & editing; Methodology; Visualization; Software; Formal analysis; Data curation.

Supporting information

Additional supporting information can be found in the online version of this article.

Supporting information.

References

Alday, A., Domingo, R., Sebastián, M., Soto, A., Aranbarri, J., González-Sampériz, P. et al. (2018) The silence of the layers: Archaeological site visibility in the Pleistocene-Holocene transition at the Ebro Basin. *Quaternary Science Reviews*, 184, 85–106.

Alday, A. (coord.) 2006. El Mesolítico de muescas y denticulados en la cuenca del Ebro y el litoral mediterráneo peninsular. Diputación Foral de Álava, Álava.

Alonso, N. & López, D. 2005. Esclerocios de *Cenococcum geophilum* Fr. En yacimientos protohistóricos del nordeste peninsular, in Molera, J., Farjas, J., P. Roura, P., Pradell, T, (Eds), Actas del VI Congreso Ibérico de Arqueometría, Girona, 213 – 221.

Andrefsky, W. (2005) *Lithics: Macroscopic Approaches to Analysis, Cambridge. ed.* Cambridge: Cambride University Press.

Aparicio, J. 2008. La necrópolis mesolítica de El Collado (Oliva-Valencia). Diputación provincial de Valencia, Valencia.

Aura, J.E., Carrión, C., Estrelles, E. & Pérez-Jordà, G. (2005) Plant economy of huntre-gatherer gropus sat the end of the last Ice Age:

plant macroremains from the cave of Santa Maira (Alacant, Spain) ca.12000-9000 B.P. *Vegetation history and Archaeobotany*, 14, 542–550.

Badal, E. (1998) El interés económico del pino piñonero para los habitantes de la Cueva de Nerja. In: Sanchidrián, J.L. & Simón, M.D., (Eds) *Las culturas del Pleistoceno superior en Andalucía*. Málaga: Patronato de la Cueva de Nerja. pp. 287–300.

Baddeley, A., Turner, R. & Rubak, E. (2015) 'spatstat': Spatial Point Pattern. *Analysis, Model-fitting, Simulation, Tests. R package version*, 1, 43–0.

Berger, J. and Guilaine, J. (2009) The 8200 cal BP abrupt environmental change and the Neolithic transition: A Mediterranean perspective. *Quaternary International*, 200, 31–49.

Berihuete Azorín, M. et al. (2017) Explotación de recursos vegetales en el Mesolítico: el sitio Parque Darwin (Madrid). In: Eraso, J.F., Mujika Alustiza, J.A., Arrizabalaga Valbuena, Á., García Diez, M. (Eds.) *Miscelánea En Homenaje a Lydia Zapata Peña (1965-2015)*. Universidad del País Vasco. pp. 83–106.

Bernabeu, J., García, O., Pardo, S., Barton, C.M. & McClure, S.B. (2014) AEA 2012 Conference Reading: Socioecological dynamics at the time of Neolithic transition in Iberia. *Environmental Archaeology*, 19, 214–225.

Bernabeu, J., García, O., Barton, M. & McClure, S. (2016) Radiocarbon dates, climatic events, and social dynamics during the Early Neolithic in Mediterranean Iberia. *Quaternary International*, 403, 201–210.

Bicho, N., Umbelino, C., Detry, C. & Pereira, T. (2010) The emergence of Muge Mesolithic shell middens in Central Portugal and the 8200 cal yr BP Cold Event. *Journal of Island and Coastal Archaeology*, 5, 86–104.

Blaauw, M. & Christen, J.A. (2011) Flexible paleoclimate age-depth models using an autoregressive gamma process. *Bayesian Anal*, 6, 457–474.

Blockley, S., Candy, I., Matthews, I., Langdon, P., Langdon, C., Palmer, A. et al. (2018) The resilience of postglacial hunter-gatherers to abrupt climate change. *Nature Ecology & Evolution*, 2, 810–818.

Bojnanský, V. & Fargašová, A. (2007) *Atlas of seEds and fruits of Central and East European flora. The Carpathian Mountains Region*. Netherlands, Dordrecht: Springer.

Bond, G., Showers, W., Cheseby, M., Lotti, R., Almasi, P., de Menocal, P.B. et al. (1997) A Pervasive Millennial-Scale Cycle in North Atlantic Holocene and Glacial Climates. *Science*, 278, 1257–1265.

Bronk Ramsey, C. (2008) Deposition models for chronological records. *Quaternary Science Reviews*, 27, 42–60.

Bronk Ramsey, C. (2009) Bayesian analysis of radiocarbon dates. *Radiocarbon*, 51(1), 337–360.

Bronk Ramsey & ,C. (2017) Methods for Summarizing Radiocarbon Datasets. *Radiocarbon*, 59, 1809–1833.

Buck, C.E., Cavanagh, W.G. & Litton, C.D. (1996) *The Bayesian Approach to Interpreting Archaeological Data*. Chichester: Wiley.

Budsky, A. *et al.* (2019) Speleothem $\delta^{13}C$ record suggests enhanced spring/summer drought in south-eastern Spain between 9.7 and 7.8 ka – A circum-Western Mediterranean anomaly? *The Holocene*, 29(7), 1113–1133.

Burjachs, F., Jones, S.E., Giralt, S. & Fernández-López de Pablo, J. (2016) Lateglacial to Early Holocene recursive aridity events in the SE Mediterranean Iberian Peninsula: The Salines playa lake case study. *Quaternary International*, 403, 187–200.

Butzer, K.W. (1982) *Archaeology as Human Ecology: Method and Theory for a Contextual Approach*. Cambridge: Cambridge University Press. https://doi.org/10.1017/CBO9780511558245

Cacho, C. & Jordá-Pardo, J.F. (2009) El Tossal de la Roca: The Pleistocene-Holocene Transition in the Mediterranean Region of Eastern Spain. *Journal of Anthropological Research*, 65, 221–236. https://doi.org/10.3998/jar.0521004.0065.204

Cacho, C., Fumanal, P., López, P., López, J.A., Pérez, M., Martínez, R. et al. (1995) El Tossal de la Roca (Vall d'Alcalà, Alicante). Reconstrucción paloeambiental y cultural de la transición del Tardiglaciar al Holoceno Inicial. *Recerques del Museu d'Alcoi*, IV, 11–101.

Cacho, I., Grimalt, J.O., Canals, M., Sbaffi, L., Shackleton, N.J., Schoenfeld, J. et al. (2001) Variability of the western Mediterranean Sea surface temperature during the last 25,000 years and its connection with the Northern Hemisphere climatic changes. *Paleoceanography*, 16, 40–52.

Canals, A. and Guerra, D. (2011) Yacimientos arqueológicos de la Sierra de Atapuerca: Un sistema inalámbrico y computerizado de registro de datos de campo. *Virtual Archaeology Review*, 2, 147–150. https://doi.org/10.4995/var.2011.4572

Canals, A., Rodríguez, J. & Sánchez, R. (2008) The 3COORsystem for data recording in archaeology. *Journal of Anthropological Sciences*, 86, 133–141.

Cappers, R.T.J., Neef, R. & Bekker, R.M. 2009. Digital Atlas of Economic Plants. Groningen Archaeological Studies 9, vol. 1. Barhuis & Groningen University Library. Groningen.

Carbonell, E., Mosquera, M., Ollé, A., Rodríguez, X.P., Sala, R., Vaquero, M. et al. 1992. New elements of the Logical Analytic System. Cahier Noir, 6. Tarragona.

Carbonell, E. & Mora, R. 1985. Anàlisi espacial d'un campament prehistòric del Post- Glacial. Sota Palou (Campdevànol). Cypsela Rev. prehistòria i protohistòria 5, 35– 45.

Casquel, T., Cerdà, A., Ferrer, C., Fumanal, M.P., Manzanares, V. & Viñals, M.J. (1989) Los depósitos cuaternarios de l'Arenal de Petrel (Alicante). *Cuadernos de Geografía*, 45, 21–34.

Chabal, L. (1988) Pourquoi et comment prélever les charbons de bois pour la période antique: les méthodes utilisées sur le site de Lattes (Hérault). *Lattara*, 1, 187–222.

Chabal, L. 1997. Forêts et sociétés en Languedoc (Néolithique final, Antiquité tardive): l'anthracologie, méthode et paléoécologie. Éditions de la Maison des Sciences de l'Homme. Documents d'archéologie française, 63. Paris.

Chabal, L., Fabre, L., Terral, J.F. & Théry-Parisot, I. 1999. L'Anthracologie, in Ferdière, A. (ed.), La Botanique. Ed. Errance, Paris, pp. 43-104.

Clark, P.J. & Evans, F.C. (1954) Distance to nearest neighbor as a measure of spatial relationships in populations. *Ecology*, 35, 445–453.

Clark, G.A. and Barton, C.M. (2022) The Mesolithic of Atlantic Coastal Spain – a comparison with the Middle Ebro Basin. *Comptes Rendus Palevol*, 21(3), 39–114.

Clark, J.S., Grimm, E.C., Donovan, J.J., Fritz, S.C., Engstrom, D.R. & Almendinger, J.E. (2002) Drought cycles and landscape responses to past aridity on prairies of the northern Great Plains, USA. *Ecology*, 83, 595–601.

Combourieu-Nebout, N., Peyron, O., Dormoy, I., Desprat, S., Beaudouin, C., Kotthoff, U. et al. (2009) Rapid climatic variability in the west Mediterranean during the last 25000 years from high resolution pollen data. *Climate of the Past*, 5, 503–521.

Cortés, M., Jiménez, F.J., Simón, M.D., Gibaja, J.F., Carvalho, A.F., Martínez, F. et al. (2012) The Mesolithic-Neolithic transition in southern Iberia. *Quaternary Research*, 77, 221–234.

CRPES. 1985. Sota Palou. Campdevànol. Un centre d'intervenció prehistòrica postglaciar a l'aire lliure. Diputació de Girona, Girona.

Crombé, P. & Langohr, R. (2020) On the origin of Mesolithic charcoal-rich pits: A comment on Huisman *et al.* 2020. *Journal of Archaeological Science*, 119, 105058.

Crombé, P., Langohr, R. & Louwagie, G. (2015) Mesolithic hearth-pits: fact or fantasy? A reassessment base don the evidence from the sites of Doel and Verrebroek (Belgium). *Journal of Archaeological Science*, 61, 158–171.

Crombé, P., Robinson, E., Van Strydonck, M. & Boudin, M. (2013) Radioacrbon dating of Mesolithic open-air sites in the coversand area of the North-West European plains: Problems and prospects. *Archaeometry*, 55, 545–562.

Dye, T.S. & Buck, C.E. (2015) Archaeological sequence diagrams and Bayesian chronological models. *Journal of Archaeological Science*, 83, 84–93.

Escobar, A. 2010. Tras las huellas del cambio en el centro peninsular. La industria de muescas y denticulados del yacimiento de Parque Darwin (Madrid) en el contexto del IX milenio BP. Universidad Autónoma de Madrid.

Fernández-López de Pablo, J. (2016) The timing of postglacial coastal adaptations in Eastern Iberia: a Bayesian chronological model for the El Collado shell midden (Oliva, Valencia, Spain). *Quaternary International*, 407, 94–105.

Fernández-López de Pablo, J., Gutiérrez-Roig, M., Gómez-Puche, M. et al. (2019) Palaeodemographic modelling supports a population bottleneck during the Pleistocene-Holocene transition in Iberia. *Nature Commun*, 10, 1872. https://doi.org/10.1038/s41467-019-09833-3

Fernández-López de Pablo, J. & Gabriel, S. (2016) El Collado shell midden and the exploitation patterns of littoral resources during the Mesolithic in the Eastern Iberian Peninsula. *Quaternary International*, 407, 106–117.

Fernández-López de Pablo, J., Ferrer, C., Gómez, M., Tormo, C. & Sanchis, A. (2015) Open-air Mesolithic sites in the Central Mediterranean region of Spain: New evidence and research directions. In: Bicho, N., Detry, C., Price, T.D. & Cunha, E. (Eds.) *Muge 150th: The 150th Anniversary of the Discovery of Mesolithic Shellmiddens—Vol. 2*. Cambridge Scholar Publishing. pp. 75–91.

Fernández-López de Pablo, J., Salazar, D.C., Subirà, M.E., Roca de Togores, C., Gómez, M., Richards, M.P. et al. (2013) Late Mesolithic burials at Casa Corona (Villena, Spain): direct radiocarbon and palaeodietary evidence of the last forager populations in Eastern Iberia. *Journal of Archaeological Science*, 40, 671–680.

Fernández-López de Pablo, J., Gómez, M., Ferre, C. & Yll, R. (2011a) El Arenal de la Virgen (Villena, Alicante), primer asentamiento perilacustre del Mesolítico de Muescas y Denticulados en la Península Ibérica: Datos culturales, cronoestratigráficos y contextualización paleoambiental. *Zephyrus LXVIII*, 87–114.

Fernández-López de Pablo, J., Gómez, M. & Martínez, A. (2011b) Systematic consumption of non-marine gastropods at open-air Mesolithic sites in the Iberian Mediterranean region. *Quaternary International*, 244, 45–53.

Fernández-López de Pablo, J. & Jochim, M. (2010) The impact of the 8,200 cal bp climatic event on human mobility strategies during the Iberian Late Mesolithic. *Journal of Anthropological Sciences*, 66, 39–68.

Fernández-López de Pablo, J., Gómez Puche, M. & Martínez-Ortí, C. (2011b) Systematic consumption of non-marine gastropods at open-air Mesolithic sites in the Iberian Mediterranean region. *Quaternary International*, 244, 45–53.

Ferrer, C. (2011) Estudio sedimentológico del yacimiento arqueológico de Benàmer. In: Torregrosa, P., Jover, F.J. & López, E. (Eds.) *Benàmer (Muro d'Alcoi, Alicante). Mesolíticos y neolíticos en las tierras meridionales valencianas. Serie de Trabajos Varios del SIP 112*. Valencia: Diputación de Valencia. pp. 65–84.

Ferrer, C. & Fumanal, M.P. 1997. Factores geomorfológicos que caracterizan la Laguna de Villena. Agua y Territorio. I Congreso de Estudios del Vinalopó. Ayunta-miento de Petrer. Ayuntamiento de Villena. Centre d' Estudis Locals de Petrer. Fundación Municipal José Maria Soler. Villena. 35-43.

Fletcher, W.J., Sánchez-Goñi, M.F., Peyron, O. & Dormoy, I. (2010) Abrupt climate changes of the last deglaciation detected in a western Mediterranean forest record. *Climate Past*, 6, 245–264.

Fortea, J. 1973. Los complejos microlaminares y geométricos del Epipaleolítico mediterráneo español. Salamanca.

Fyfe, R.M., Woodbridge, J., Palmisano, A. *et al.* (2019) Prehistoric palaeodemographics and regional land cover change in eastern Iberia. *The Holocene*, 29(5), 799–815.

García-Puchol, O. & Aura, J.E. (2006) *El Abric de la Falguera (Alcoi, Alacant). 8000 años de ocupación humana en la cabecera del riu Alcoi*. Alicante: Diputación de alicante, Ayuntamiento de Alcoi y Caja de Ahorros del Mediterráneo.

García Atiénzar, G., Jover, F.J., Ibáñez, C., Navarro, C. & Andrés, D. (2006) El yacimiento neolítico de la calle Colón (Novelda, Alicante). *Recerques del Museu d'Alcoi*, 15, 19–28.

García-Escárzaga, A., Gutiérrez-Zugasti, I., Marín-Arroyo, A.B. *et al.* (2022) Human forager response to abrupt climate change at 8.2 ka on the Atlantic coast of Europe. *Science Reports*, 12, 6481. https://doi.org/10.1038/s41598-022-10135-w

García-Martínez de Lagrán, I. *et al.* (2016) 8.2 ka BP paleoclimatic event and the Ebro Valley Mesolithic groups: Preliminary data from Artusia rock shelter (Unzué, Navarra, Spain). *Quaternary International*, 403, 151–173. https://doi.org/10.1016/j.quaint.2015.06.050

Gibaja, J.F., Subirà, M.E., Terradas, X., Santos, F.J., Agulló, L., Gómez-Martínez, I. et al. (2015) The Emergence of Mesolithic Cemeteries in SW Europe: Insights from the El Collado (Oliva, Valencia, Spain) Radiocarbon Record. *PLoS One*, 10, e0115505.

Giralt, S., Burjachs, F., Roca, J.R. & Julià, R. (1999) Late Glacial to Early Holocene environmental adjustment in the Mediterranean semi-arid zone of the Salines playa-lake (Alacant, Spain). *Journal of Paleolimnology*, 21, 449–460.

Gómez-Puche, M. and Fernández López de Pablo, J. (2016) El yacimiento Neolítico del Arenal de la virgen (Villena, Alicante). *Estudio de la colección de materiales de Josñe María Soler. Bilyana*, 1, 17–30.

González-Sampériz, P., Utrilla, P., Mazo, C., Valero-Garcés, B., Sopena, M., Morellón, M. et al. (2009) Patterns of human occupation during the early Holocene in the Central Ebro Basin (NE Spain) in response to the 8.2 ka climatic event. *Quaternary Research*, 71, 121–132.

Grootes, P.M. & Stuiver, M. (1997) Oxygen 18/16 variability in Greenland snow and ice with 103- to 105-year time resolution. *J. Geophys. Res. Oceans*, 102, 26455–26470.

Harris, E.C. (1989) *Principles of Archaeological Stratigraphy*. London: Academic Press.

Hernek, R. (2003) A Mesolithic Winter site with a Sunken Dwelling from the Swedish west coast. In Larsson, L., Kindgren, H., Knutsson, K., Loeffler, D., Akerlund, A. (Eds.) Mesolithic on the Move. Papers presented at the Sixth International Conference on the Mesolithic in Europe, Stockholm 2000. p. 222-229.

Inizan, M.L., Reduron-Ballinger, M., Roche, H. & Tixier, J. 1999. Terminology and Technology of Knapped Stone. Cercle de Recherches et d'Etudes Préhistoriques (CREP), Meudon.

Jones, S.E., Burjachs, F., Ferrer, C., Giralt, S., Schulte, L. & Fernández-López de Pablo, J. (2018) A multi-proxy approach to understanding complex responses of salt-lake catchments to climate variability and human pressure: A Late Quaternary case study from south-eastern, Spain. *Quaternary Science Reviews*, 184, 201–223.

Torregrosa, P., Jover, F.J. & López, E. 2011. Benàmer (Muro d'Alcoi, Alicante). Mesolíticos y neolíticos en las tierras meridionales valencianas. Serie de Trabajos Varios del SIP 112. Diputación de Valencia. Valencia.

Julià, R., Burjachs, F., Dasí, M.J., Mezquita, F., Miracle, M.R., Roca, J.R. et al. (1998) Meromixis origin and recent trophic evolution in the Spanish mountain lake La Cruz. *Aquatic Sciences*, 60, 279–299.

Julià, R., Negendank, J.F.W., Seret, G., Brauer, A., Burjachs, F., Endres, C. et al. 1994. Holocene climatic change and desertification in Western Mediterranean, in: Terra Nostra. Climate dynamics recorded in long continental high resolution time series since the last interglacial. Schriften der Alfred-Wegener-Stiftung), 1/94, 81-84.

Martí, B., Aura, J.E., Juan-Cabanilles, J., García Puchol, O. & Ferández, J. (2009) El mesolítico Geométrico de tipo«Cocina» en el País Valenciano. In: Utrilla, P. & Montes, L. (Eds.) *El Mesolítico Geométrico en la Península Ibérica. Monografías Arqueológicas*. Zaragoza: Universidad de Zaragoza. pp. 205–258.

Martinez-Moreno, J. & Mora, R. 2011. Spatial organization at Font del Ros, a Mesolithic settlement in the south-eastern Pyrenees, in: Gaudzinski-Windheuser, S., Jöris, O., Sensburg, M., Street, M., Turner, E. (Eds.), Site-Internal Spatial Organization of Hunter-Gatherer Societies: Case Studies from the European Palaeolithic and Mesolithic. RGZM, Mainz, pp. 213–231.

Martínez-Varea, C.M. (2016) "Si bien buscas encontrarás". Metodología para el análisis carpológico del Magdaleniense medio de la Cova de les Cendres (Teulada-Moraira, Alicante). *Pyrenae*, 47, 73–93.

Martins, J., Carvalho, A. & Soares, A. (2008) A calibraçao das datas de radiocarbono dos esqueletos de Muge. *Promontoria*, 6, 73–93.

McLaughlin, T.R., Gómez-Puche, M., Cascalheira, J., Bicho, N. & Fernández-López de Pablo, J. (2021) Late Glacial and Early Holocene human demographic responses to climatic and environmental change in Atlantic Iberia. *Philosophical Transactions of the Royal Society B*, 376, 20190724. https://doi.org/10.1098/rstb.2019.0724

Montes, L., Domingo, R., González-Sampériz, P., Sebastián, M. *et al.* (2016) Landscape, re- sources and people during the Mesolithic and Neolithic times in NE Iberia: the Arba de Biel Basin. *Quaternary International*, 403, 133e150. https://doi.org/10.1016/j.quaint.2015.05.041

Peeters, H. & Niekus, M.J.L.T.h. 2017. Mesolithic pit hearths in the northern Netherlands. Function, time-depth, and behavioural context. In: Achard-Corompt, N., Ghesquière, E., Riquier, V.

(Eds.), Creuser au Mésolithique/Digging in the Mesolithic. Actes de la séance de la Société préhistorique française de Châlons-en-Champagne (29-30 mars 2016). Paris, Société préhistorique française, 2017 (Séances de la Société préhistorique française, 12), pp. 225–239.

Polo-Díaz, A., Rabuñal, J.R., Guérin, G. and Fernández-López de Pablo, J. 2022. "Mesolithic Hearth-pits and Formation Processes: A Geoarchaeological Investigation of Sediments from El Arenal De La Virgen Site (SE Iberia)." SocArXiv. June 6. https://doi.org/10.31235/osf.io/86tqz.

R Core Team. 2020. R: A Language and Environment for Statistical Computing. R Foundation for Statistical Computing, Vienna, Austria. https://www.R-project.org/.

Rabuñal, J.R. 2021. Análisis de la distribución espacial y estudio morfo-técnico de la industria lítica de los yacimientos mesolíticos de El Arenal de la Virgen y Casa Corona (Villena, Alicante). Unpublished PhD thesis, University of Alicante.

Rabuñal, J.R. & Fernández-López de Pablo, J. 2022. Expedient microlithic production in the Notched and Denticulated Mesolithic in the Iberian Mediterranean region. Insights from the open-air site of Arenal de la Virgen (Villena, Alicante). State of the Art - Advances in the study of Palaeolithic and Mesolithic creative behaviour. Booklet of the 63rd Annual Meeting of the Hugo Obermaier Society. pp. 75 - 76. 2022. ISBN 978-3-946387-41-1

Rasmussen, S.O., Bigler, M., Blockley, S.P., Blunier, T., Buchardt, S.L., Clausen, H.B. et al. (2014) A stratigraphic framework for abrupt climatic changes during the Last Glacial period based on three synchronized Greenland ice-core records: refining and extending the INTIMATE event stratigraphy. *Quaternary Science Reviews*, 106, 14–28.

Reimer, P.J. *et al.* (2020) The IntCal20 Northern Hemisphere Radiocarbon Age Calibration Curve (0-55 cal kBP). *Radiocarbon*, 62(4), 725–757.

Roca, J.R. & Julià, R. (1997) Late-glacial and Holocene lacustrine evolution based on ostracode assemblages in southeastern Spain. *Geobios*, 30(6), 823–830.

Roda Gilabert, X., Martínez-Moreno, J. & Torcal, R.M. (2016) Ground stone tools and spatial organization at the Mesolithic site of font del Ros (southeastern Pre- Pyrenees, Spain. *Journal of Archaeological Science Reports.* https://doi.org/10.1016/j.jasrep.2015.11.023

Rohling, E.J. & Pälike, H. (2005) Centennial-scale climate cooling with a sudden cold event around 8,200 years ago. *Nature*, 434, 975–979.

Rolfsen, P. (1980) Disturbance of archaeological layers by processes in the soil. *Norwegian Archaeological Review*, 13, 111–118. https://doi.org/10.1080/00293652.1980.9965336

Schiffer, M.B. (1987) *Formation Processes of the Archaeological Record.* Albuquerque: University of New Mexico Press.

Schweingruber, F.H. 1990. Anatomy of European woods: An Atlas for the identification of European trees. Verlag Kessel. Bern.

Soler, J.M.ª., 1965: "El Arenal de la Virgen y el neolítico cardial de la comarca villenense". Villena 15: s/p.

Stuiver, M., Grootes, P.M. & Braziunas, T.F. (1995) The GISP2 -18O Climate Record of the Past 16,500 Years and the Role of the Sun, Ocean and Volcanoes. *Quaternary Research*, 44, 341–354.

Torregrosa, P., Jover, F.J. & López, E. 2011. Benàmer (Muro d'Alcoi, Alicante). Mesolíticos y neolíticos en las tierras meridionales valencianas. Serie de Trabajos Varios del SIP 112. Diputación de Valencia. Valencia.

Utrilla, P. *et al.* (2009) El Mesolítico geométrico en Aragón. In: Utrilla, P., Montes, L. (Eds.) *El Mesolítico Geométrico En La Península Ibérica*. Zaragoza: Universidad de Zaragoza. pp. 131–190.

Van Der Schriek, T.D. *et al.* (2008) Holocene palaeoecology and floodplain evo- lution of the Muge tributary, Lower Tagus basin, Portugal, *Quaternary International*, 189, pp. 135–151.

Vernet, J.-L., Bazile, E. & Evin, J. (1979) Coordination des analyses anthracologiques et des datations absolues sur charbons de bois. *Bulletin de la Société Préhistorique Française*, 76, 76–79.

Verjux, C.h. (2003). The function of the Mesolithic sites in the Paris basin (France). New data. In Larsson, L., Kindgren, H., Knutsson, K., Loeffler, D., Akerlund, A. (Eds.) Mesolithic on the Move. Papers presented at the Sixth International Conference on the Mesolithic in Europe, Stockholm 2000. P. 262-268.

Vidal-Matutano, P., Hernández, C.M., Galván, B. & Mallol, C. (2015) Neanderthal firewood management: evidence from Stratigraphic Unit IV of Abric del Pastor (Eastern Iberia). *Quaternary Science Reviews*, 111,81–93.

Villa, P. & Courtin, J. (1983) The interpretation of stratified sites: A view from underground. *Journal of archaeological science*, 10, 267–281. https://doi.org/10.1016/0305-4403(83)90011-0

Waddington, C. *et al.* 2003. A Mesolithic settlement site at Howick, Northumberland: a preliminary report. Archaeologia Aeliana 5th Series, 32: 1–12.

Wood, W.R. & Johnson, D.L. (1978) A Survey of Disturbance Processes in Archaeological Site Formation. In: Schiffer, M.B., (ed) *Advances in Archaeological Method and Theory*, 1. San Diego: Academic Press. pp. 315–381.

Yanes, Y. & Fernández-Lopez-de-Pablo, J. (2017) Calibration of the stable isotope composition and body size of the arid-dwelling land snail Sphincterochila candidissima, a climatic archive abundant in Mediterranean archaeological deposits. *The Holocene*, 27, 890–899. https://doi.org/10.1177/0959683616675943

Zielhofer, C., Fletcher, W.J., Mischke, S., De Batist, M., Campbell, J.F.E., Joannin, S. et al. (2017) Atlantic forcing of Western Mediterranean winter rain minima during the last 12,000 years. *Quaternary Science Reviews*, 157, 29–51.

Zilhão, J. (2003) Algumas observações acerca do Mesolítico do interior peninsular e do modelo de passagem ao Neolítico através de colonização pioneira por via marítima. Comentario a Carvalho, 2007. *O Arqueólogo Portugues 4*, 21, 108–118.

Zilhão, J. (1998) A passagem do Mesolítico ao Neolítico na costa do Alentejo. *Revista portuguesa de arqueologia*, 1, 27–44.

